Elsevier Editorial System(tm) for BBA - Biomembranes
Manuscript Draft

Manuscript Number: BBAMEM-12-105R1

Title: Atomic force microscopy imaging of lipid rafts of human breast cancer cells

Article Type: Regular Paper

Keywords: lipid rafts
Atomic Force Microscopy
MDA-MB-231 cancer cells.

Corresponding Author: Dr Francesco Orsini, Ph.D.

Corresponding Author's Institution: Università degli Studi di Milano

First Author: Francesco Orsini, Dr

Order of Authors: Francesco Orsini, Dr; Andrea Cremona, Dr; Paolo Arosio, Dr; Paola A Corsetto, Dr; Gigliola Montorfano; Alessandro Lascialfari, Prof; Angela M Rizzo, Dr

Abstract: Several studies suggest that the plasma membrane is composed of micro-domains of saturated lipids that segregate together to form lipid rafts. Lipid rafts have been operationally defined as cholesterol- and sphingolipid-enriched membrane micro-domains resistant to solubilisation by non-ionic detergents at low temperatures. Here we report a biophysical approach aimed at investigating lipid rafts of MDA-MB-231 human breast cancer cells by coupling an Atomic Force Microscopy (AFM) study to biochemical assays namely Western Blotting and High Performance Thin Layer Chromatography. Lipid rafts were purified by ultracentrifugation on discontinuous sucrose gradient using extraction with Triton X-100. Biochemical analyses proved that the fractions isolated at the 5% and 30% sucrose interface (fractions 5 and 6) have an higher content of cholesterol, sphingomyelin and flotillin-1 with respect to the other purified fractions. Tapping mode AFM imaging of fraction 5 showed membrane patches whose height corresponds to the one awaited for a single lipid bilayer as well as the presence of micro-domains with lateral dimensions in the order of a few hundreds of nanometers. In addition, an AFM study using specific antibodies suggests the presence, in these micro-domains, of a characteristic marker of lipid rafts, the protein flotillin-1.

Response to Reviewers: Note on the referees'comments

Referee 1 Comments:

1) page 2: The "hypothesis" of the existence of rafts is not that recent (1997).

Response to Reviewer comment No. 1
We thank the referee and we have modified the text (Introduction) in the revised manuscript accordingly.

2) page 2: I don't think that monitoring the motion or the partitioning of fluorescence probes are DIRECT evidence for the existence of rafts.

Response to Reviewer comment No. 2

As suggested by the referee, we removed this sentence in the revised manuscript.

3) page 2: "...of a few hundreds nanometers...". I think that the current view of the raft domains evidence raft size of ten to tens of nanometer in size.

Response to Reviewer comment No. 3
We removed the sentence in the revised manuscript.

4) page 2: Transmission Electron Microscopy cannot assess raft structure. This has nothing to do with resolution. It is due to the fact that density differences are "probed" by the electrons, and therefore specific lipids have almost no contrast compared to other lipids or (flat) membrane proteins. On the other hand, the novel high-resolution optical microscopy techniques are powerful in the field. PALM/STORM/STED. The authors seem neglecting these aspects.

Response to Reviewer comment No. 4
We agree with the referee comment and changed the sentence at pag 2 (Introduction) in the revised manuscript adding, as suggested, considerations related to the application of novel super resolution optical microscopy techniques to the study of lipid rafts topic.

5) page 3: "...kindly provided by Dr P Degan..." is not a reproducible Method.

Response to Reviewer comment No. 5
We thank the referee and we have modified the text (Materials and Methods) in the revised manuscript.

6) page 6: The paragraph about AFM observing in aqueous environment is redundant from the introduction.

Response to Reviewer comment No. 6
We agree with the referee comment and removed the paragraph in the revised manuscript.

7) page 6: Figure 4, Section analyses are missing

Response to Reviewer comment No. 7
As suggested by the referee, we performed the rms surface roughness analysis and the experimental data have been introduced in the revised manuscript (Results).

8) page 6, page 7, figures 3, 4, 5, 7: The problem is that the raft purification protocol using the Triton should result in the raft domains. As the author state, that this is basically how they are defined, membrane domains of nanometer size that are not solubilized during soft detergent treatment. Therefore the finding of membrane patches of 1-3μm in size is worrying and indicates that we are actually not looking at the "raft fraction".

Response to Reviewer comment No. 8
Classical preparation of lipid rafts uses 1% Triton X-100 to extract whole cells and successive separation of the solubilised membranes on 5%-30% sucrose density gradient. Recently, different methods have been developed using a variety of other detergents or with detergent free techniques (Biophys J. 2011 Nov 16;101(10):2417-25. Measurement of lipid nanodomain (raft) formation and size in sphingomyelin/POPC/cholesterol vesicles shows TX-100 and transmembrane helices increase domain size by coalescing preexisting nanodomains but do not induce domain formation. Pathak P, London E).

Some observations raised the hypothesis that extraction of cells with detergents may be generating clusters of raft lipids and proteins that did not exist in the intact cells.
Our data showed in fraction 5 the presence of membrane patches of 1-3 μm that may be formed through a mechanism of coalescence as a result of detergent treatment. Nevertheless recent data demonstrated that TX-100 does not induce domain formation or increase the fraction of the bilayer in the ordered state, although it does increase domain size by coalescing preexisting domains (Biophys J. 2011 Nov 16;101(10):2417-25. Measurement of lipid nanodomain (raft) formation and size in sphingomyelin/POPC/cholesterol vesicles shows TX-100 and transmembrane helices increase domain size by coalescing preexisting nanodomains but do not induce domain formation. Pathak P, London E). Thus our observations are in agreement with this theory. We added these considerations in the revised manuscript (Discussion and Conclusions).

9) figure 4: The two domains labeled 3 are clearly different. One is flat and smooth and does clearly not contain potential proteins, the other is corrugated and fuzzy and does contain rough molecules.

Response to Reviewer comment No. 9
Really, the two microdomains labelled 3 in figure 4 exhibit a surface roughness as suggested by their corrugated appearance in AFM image (white spots). These microdomains are protruding from the membrane lipid bilayer, labelled 2, which has a very smooth surface. In any case, we performed the rms surface roughness analysis of these regions and the experimental data have been introduced in the revised manuscript (Results).

10) figure 5 and 6 (with respect to above comment): The domain in figure 5 is clearly different from domain shown in 6. The statement that there are proteins, appears as an overstatement.

Response to Reviewer comment No. 10
The different appearance of the two microdomains visualized in Fig. 5 and Fig. 6 is mainly related to the different dimensions of the scan areas and z range in the two figures. In particular, visualizing a smaller scan area the corrugated and fuzzy appearance of the microdomain surface appears to be better defined (Fig. 6; scan area = 200x200 nm2; vertical scale = 2 nm) than scanning a bigger area (Fig. 5; scan area = 1.6x1.6 μm2; vertical scale = 20 nm). Really, the microdomains exhibit a similar surface roughness as proved by the rms surface roughness analysis that has been introduced in the revised manuscript (Results).

11) figure 7: There is a worrying region in the middle of the right panel. It appears like uncontrolled forces are applied. The "normal" lipid patch in the middle right of the image is about 2 times larger in the right panel compared to the left. Antibody binding should result mainly in an increase of height and roughness of the domains (rather than enlargement), see antibody labeling of bacteriorhodopsin, 1996.

Response to Reviewer comment No. 11
Following the suggestion of the referee we performed the height profile analysis as well as the rms surface roughness analysis of the microdomains before and after the antibody treatment. Moreover, we repeated the antiboby experiment using as control experiment a non-specific antibody (anti clathrin hc, an antibody raised against a non raft protein marker) to get rid of possible physisorption phenomena. New AFM topography images as well as experimental data obtained by the above described analyses have been introduced in the revised manuscript (Results). Moreover we would like to point out that in literature there are also works where the protein antibody labelling has been studied by AFM valuating the surface area increase (N Buzhynskyy, C Salesse and S Scheuring, Rhodopsin is spatially heterogeneously distributed in rod outer segment disk membranes, J. Mol. Recognit. 2011; 24: 483–489).

Referee 2 Comments:

1) The authors claim that AFM has the advantage of not requiring invasive sample preparation, at variance with EM, and other techniques. Nevertheless, the procedure followed for getting the various fractions to be studied by AFM exposes membranes to environments that are quite far from the physiologic one. The authors should comment on the impact of their sample preparation on the retrieval of physiologically revenant information about lidip rafts.

Response to Reviewer comment No. 1
We agree with the referee comment. In particular, we would like to point out that AFM requires sample preparation conditions less invasive in comparison to other microscopy techniques where staining, dehydration, and UHV are often needed. Nevertheless we are aware that the lipid raft purification protocol followed in the work exposes membranes to an environment quite far from the physiological one. We introduced these considerations in the revised manuscript (Discussion and Conclusions).

2) Do the authors have a control over the membrane patch orientation at surface? This aspect is of course of main importance in assessing the presence of micro-domains by AFM.

Response to Reviewer comment No. 2
Really, the sample preparation protocol for AFM imaging we developed and used in the present work does not allow us to select the orientation of the membrane patches visualized on the mica support. We introduced this consideration in the revised manuscript and this point has been taken in account in the interpretation of the experimental data (Results; Discussion and Conclusions).

3) i) How can the authors be sure that an AB suitable for WB can be used also in more native conditions on transmembrane proteins, since many domains (and the N-terminal domain of flotillin-1 is not an exception) are membrane embedded?

Response to Reviewer comment No. 3
We agree with the referee comment. Unfortunately for a mistake we reported in the text an incorrect information. Really in the AB experiment we used a rabbit polyclonal AB raised against amino acids 324-427 of flot-1 (Santa Cruz Biotechnology), protein segment which is near its C-terminus and fully exposed in the cytoplasmic side of the plasma membrane. We changed the incorrect sentence in the revised manuscript (Results).

4) ii) The authors define as "specific" the AB binding they get on their micro-domains, but they do not demonstrate any specificity. The control experiment without the AB is not informative in that sense. To demonstrate specificity, two more measurements should be performed i.e. a similar measurements with a non-specific AB, to get rid of possible physisorption phenomena; and an experiment with blockers (e.g peptides) which can compete with "specific" AB for binding the same epitope on flotillin-1. Otherwise, I think that any statement derived from experiments with AB and AFM has to be markedly weakened.

Response to Reviewer comment No. 4
As suggested by the referee we performed a new AB experiment. In particular, the anti flot-1 experiment gave results fully comparable with the ones reported in the text. Moreover, to demonstrate specificity and get rid of possible physisorption phenomena we used as control experiment a non specific AB, the anti clathrin HC a mouse monoclonal antibody raised against the N-terminus of clathrin heavy chain (Santa Cruz Biotechnology) a non raft protein marker. New AFM topography images as well as experimental data have been introduced in the revised manuscript (Results). The suggested experiment using blockers is surely very relevant from the biochemical point of view but it appears not

fully useful applying the AFM technique. In fact, AFM detects the antibody binding mainly as an enlargement of the microdomain surface area. Peptides could induce an increase of the microdomain surface area not easily noticeable from the effect produced by anti flot-1.

5) pg. 3 "Tubes were centrifuged at 40000 rpm for 17 h at 4 °C in a Ultracentrifuge (Beckman Coulter)." The "g" equivalent must be provided (or the rotor diameter) in order to make the procedure repeatable.

Response to Reviewer comment No. 5
We thank the referee and we have modified the text in the revised manuscript accordingly.

6) pg. 4 "Free CHOL and SM were quantified by HP-TLC with hexane/ether/glacial acetic acid (90:10:1 by volume) and with chloroform/methanol/glacial acetic acid/water (60:45:4:2 by volume)," Please, either use "/" or ":" in the sentence.

Response to Reviewer comment No. 6
In the revised manuscript the text has been changed as suggested.

Milan, June 14th, 2012

Dear Professor Yechiel Shai,

We here submit a new version of our paper entitled "Atomic force microscopy imaging of lipid rafts of human breast cancer cells" by F.Orsini, A.Cremona, P.Arosio, P.A.Corsetto, G. Montorfano, A.Lascialfari, A.M.Rizzo (*Manuscript No.: BBAMEM-12-105)*

According to the referee comments, we carried out new experiments as well as more detailed quantitative analyses in order to improve the quality of the results and better clarify the applied methodologies.

In particular, the new version includes:

- the root-mean-square (rms) surface roughness analysis of membrane patches as well as of membrane micro-domains to quantify their surface corrugation.
- A new antibody experiment. Moreover, to demonstrate specificity and get rid of possible physisorption phenomena we used as control experiment a non specific antibody (anti clathrin HC monoclonal antibody) raised against a non raft protein marker. New AFM topography images as well as experimental data have been introduced in the revised manuscript. In particular, we performed the height profile analysis as well as the rms surface roughness analysis of the membrane micro-domains before and after the antibody treatment.
- As requested from referees, the introduction has been modified to include examples of novel high-resolution optical microscopy techniques to the study of lipid raft topic.

Finally, we extensively revised the paper taking into account all the objections and the suggestions expressed by the two referees, to whom we would like to express our warmest thanks for their contribution. We therefore hope that the resulting substantially new paper we are sending you, could now be considered for the publication in your journal.

With best regards,

Francesco Orsini, PhD
Physics Dept.
University of Milan
Via Celoria, 16
20133, Milano (Italy)
Phone: +39 02 50315796
Fax: +39 02 50315775
Email: francesco.orsini@unimi.it

Atomic force microscopy imaging of lipid rafts of human breast cancer cells
Francesco Orsini, Andrea Cremona, Paolo Arosio, Paola A Corsetto, Gigliola Montorfano, Alessandro Lascialfari, Angela M Rizzo.
Manuscript No.: BBAMEM-12-105

Note on the referees'comments

Referee 1 Comments:

1) page 2: The "hypothesis" of the existence of rafts is not that recent (1997).
We thank the referee and we have modified the text (Introduction) in the revised manuscript accordingly.

2) page 2: I don't think that monitoring the motion or the partitioning of fluorescence probes are DIRECT evidence for the existence of rafts.
As suggested by the referee, we removed this sentence in the revised manuscript.

3) page 2: "...of a few hundreds nanometers...". I think that the current view of the raft domains evidence raft size of ten to tens of nanometer in size.
We removed the sentence in the revised manuscript.

4) page 2: Transmission Electron Microscopy cannot assess raft structure. This has nothing to do with resolution. It is due to the fact that density differences are "probed" by the electrons, and therefore specific lipids have almost no contrast compared to other lipids or (flat) membrane proteins. On the other hand, the novel high-resolution optical microscopy techniques are powerful in the field. PALM/STORM/STED. The authors seem neglecting these aspects.
We agree with the referee comment and changed the sentence at pag 2 (Introduction) in the revised manuscript adding, as suggested, considerations related to the application of novel super resolution optical microscopy techniques to the study of lipid rafts topic.

5) page 3: "...kindly provided by Dr P Degan..." is not a reproducible Method.
We thank the referee and we have modified the text (Materials and Methods) in the revised manuscript.

6) page 6: The paragraph about AFM observing in aqueous environment is redundant from the introduction.
We agree with the referee comment and removed the paragraph in the revised manuscript.

7) page 6: Figure 4, Section analyses are missing
As suggested by the referee, we performed the rms surface roughness analysis and the experimental data have been introduced in the revised manuscript (Results).

8) page 6, page 7, figures 3, 4, 5, 7: The problem is that the raft purification protocol using the Triton should result in the raft domains. As the author state, that this is basically how they are defined, membrane domains of nanometer size that are not solubilized during soft detergent treatment. Therefore the finding of membrane patches of 1-3µm in size is worrying and indicates that we are actually not looking at the "raft fraction".

Classical preparation of lipid rafts uses 1% Triton X-100 to extract whole cells and successive separation of the solubilised membranes on 5%-30% sucrose density gradient. Recently, different methods have been developed using a variety of other detergents or with detergent free techniques (Biophys J. 2011 Nov 16;101(10):2417-25. Measurement of lipid nanodomain (raft) formation and size in sphingomyelin/POPC/cholesterol vesicles shows TX-100 and transmembrane helices increase domain size by coalescing preexisting nanodomains but do not induce domain formation. Pathak P, London E).

Some observations raised the hypothesis that extraction of cells with detergents may be generating clusters of raft lipids and proteins that did not exist in the intact cells.

Our data showed in fraction 5 the presence of membrane patches of 1-3 µm that may be formed through a mechanism of coalescence as a result of detergent treatment. Nevertheless recent data demonstrated that TX-100 does not induce domain formation or increase the fraction of the bilayer in the ordered state, although it does increase domain size by coalescing preexisting domains (Biophys J. 2011 Nov 16;101(10):2417-25. Measurement of lipid nanodomain (raft) formation and size in sphingomyelin/POPC/cholesterol vesicles shows TX-100 and transmembrane helices increase domain size by coalescing preexisting nanodomains but do not induce domain formation. Pathak P, London E). Thus our observations are in agreement with this theory. We added these considerations in the revised manuscript (Discussion and Conclusions).

9) figure 4: The two domains labeled 3 are clearly different. One is flat and smooth and does clearly not contain potential proteins, the other is corrugated and fuzzy and does contain rough molecules.

Really, the two microdomains labelled 3 in figure 4 exhibit a surface roughness as suggested by their corrugated appearance in AFM image (white spots). These microdomains are protruding from the membrane lipid bilayer, labelled 2, which has a very smooth surface. In any case, we performed the rms surface roughness analysis of these regions and the experimental data have been introduced in the revised manuscript (Results).

10) figure 5 and 6 (with respect to above comment): The domain in figure 5 is clearly different from domain shown in 6. The statement that there are proteins, appears as an overstatement.

The different appearance of the two microdomains visualized in Fig. 5 and Fig. 6 is mainly related to the different dimensions of the scan areas and z range in the two figures. In particular, visualizing a smaller scan area the corrugated and fuzzy appearance of the microdomain surface appears to be better defined (Fig. 6; scan area = 200x200 nm^2; vertical scale = 2 nm) than scanning a bigger area (Fig. 5; scan area = 1.6x1.6 μm^2; vertical scale = 20 nm). Really, the microdomains exhibit a similar surface roughness as proved by the rms surface roughness analysis that has been introduced in the revised manuscript (Results).

11) figure 7: There is a worrying region in the middle of the right panel. It appears like uncontrolled forces are applied. The "normal" lipid patch in the middle right of the image is about 2 times larger in the right panel compared to the left. Antibody binding should result mainly in an increase of height and roughness of the domains (rather than enlargement), see antibody labeling of bacteriorhodopsin, 1996.

Following the suggestion of the referee we performed the height profile analysis as well as the rms surface roughness analysis of the microdomains before and after the antibody treatment. Moreover, we repeated the antiboby experiment using as control experiment a non-specific antibody (anti clathrin hc, an antibody raised against a non raft protein marker) to get rid of possible physisorption

phenomena. New AFM topography images as well as experimental data obtained by the above described analyses have been introduced in the revised manuscript (Results). Moreover we would like to point out that in literature there are also works where the protein antibody labelling has been studied by AFM valuating the surface area increase (N Buzhynskyy, C Salesse and S Scheuring, Rhodopsin is spatially heterogeneously distributed in rod outer segment disk membranes, J. Mol. Recognit. 2011; 24: 483–489).

Referee 2 Comments:

1) The authors claim that AFM has the advantage of not requiring invasive sample preparation, at variance with EM, and other techniques. Nevertheless, the procedure followed for getting the various fractions to be studied by AFM exposes membranes to environments that are quite far from the physiologic one. The authors should comment on the impact of their sample preparation on the retrieval of physiologically revenant information about lidip rafts.
We agree with the referee comment. In particular, we would like to point out that AFM requires sample preparation conditions less invasive in comparison to other microscopy techniques where staining, dehydration, and UHV are often needed. Nevertheless we are aware that the lipid raft purification protocol followed in the work exposes membranes to an environment quite far from the physiological one. We introduced these considerations in the revised manuscript (Discussion and Conclusions).

2) Do the authors have a control over the membrane patch orientation at surface? This aspect is of course of main importance in assessing the presence of micro-domains by AFM.
Really, the sample preparation protocol for AFM imaging we developed and used in the present work does not allow us to select the orientation of the membrane patches visualized on the mica support. We introduced this consideration in the revised manuscript and this point has been taken in account in the interpretation of the experimental data (Results; Discussion and Conclusions).

3) i) How can the authors be sure that an AB suitable for WB can be used also in more native conditions on transmembrane proteins, since many domains (and the N-terminal domain of flotillin-1 is not an exception) are membrane embedded?
We agree with the referee comment. Unfortunately for a mistake we reported in the text an incorrect information. Really in the AB experiment we used a rabbit polyclonal AB raised against amino acids 324-427 of flot-1 (Santa Cruz Biotechnology), protein segment which is near its C-terminus and fully exposed in the cytoplasmic side of the plasma membrane. We changed the incorrect sentence in the revised manuscript (Results).

4) ii) The authors define as "specific" the AB binding they get on their micro-domains, but they do not demonstrate any specificity. The control experiment without the AB is not informative in that sense. To demonstrate specificity, two more measurements should be performed i.e. a similar measurements with a non-specific AB, to get rid of possible physisorption phenomena; and an experiment with blockers (e.g peptides) which can compete with "specific" AB for binding the same epitope on flotillin-1. Otherwise, I think that any statement derived from experiments with AB and AFM has to be markedly weakened.
As suggested by the referee we performed a new AB experiment. In particular, the anti flot-1 experiment gave results fully comparable with the ones reported in the text. Moreover, to demonstrate specificity and get rid of possible physisorption phenomena we used as control experiment a non specific AB, the anti clathrin HC a mouse monoclonal antibody raised against the N-terminus of clathrin heavy chain (Santa Cruz Biotechnology) a non raft protein marker. New AFM topography images as well as experimental data have been introduced in the revised

manuscript (Results). The suggested experiment using blockers is surely very relevant from the biochemical point of view but it appears not fully useful applying the AFM technique. In fact, AFM detects the antibody binding mainly as an enlargement of the microdomain surface area. Peptides could induce an increase of the microdomain surface area not easily noticeable from the effect produced by anti flot-1.

5) pg. 3 "Tubes were centrifuged at 40000 rpm for 17 h at 4 °C in a Ultracentrifuge (Beckman Coulter)." The "g" equivalent must be provided (or the rotor diameter) in order to make the procedure repeatable.
We thank the referee and we have modified the text in the revised manuscript accordingly.

6) pg. 4 "Free CHOL and SM were quantified by HP-TLC with hexane/ether/glacial acetic acid (90:10:1 by volume) and with chloroform/methanol/glacial acetic acid/water (60:45:4:2 by volume)," Please, either use "/" or ":" in the sentence.
In the revised manuscript the text has been changed as suggested.

Graphical Abstract (for review)

TM-AFM Image of a membrane micro-domain (1) protruding by 1 nm from the surface of a membrane patch (2) of MDA-MB-231 human breast cancer cells

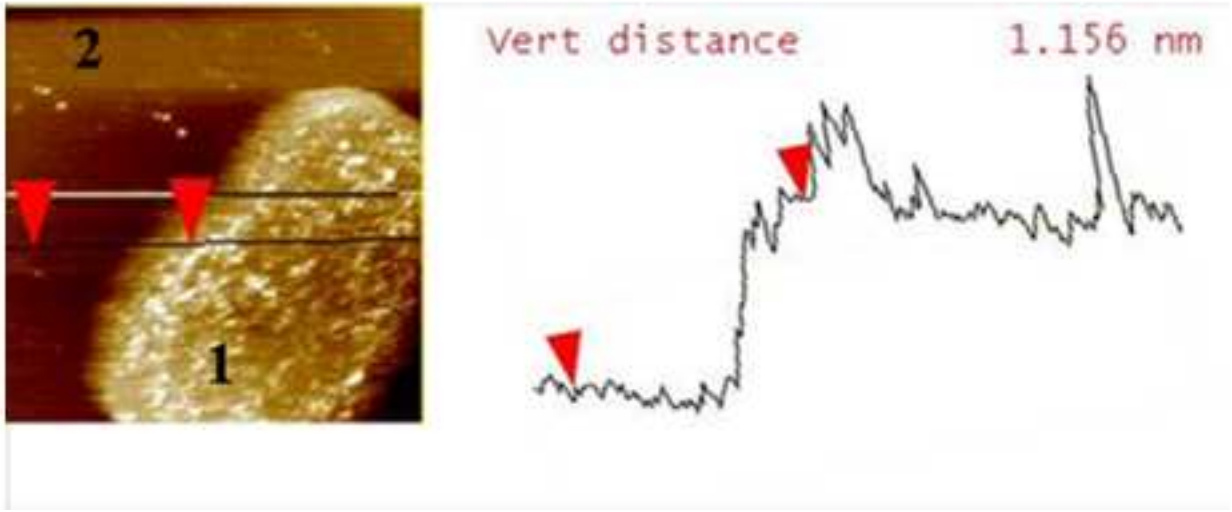

***Highlights (for review)**

- Lipid rafts of MDA-MB-231 cancer cells were studied by AFM and biochemical assays.
- AFM showed membrane micro-domains with lateral sizes of a few hundreds of nm.
- WB and HP-TLC detected an high CHOL, SM and Flot-1 content in the micro-domains.
- AFM study using specific antibodies identified Flot-1 in the micro-domains.

Atomic force microscopy imaging of lipid rafts of human breast cancer cells

[1]F.Orsini*, [2]A.Cremona*, [1]P.Arosio, [2]P.A.Corsetto, [2]G. Montorfano, [1,3]A.Lascialfari, [2]A.M.Rizzo

[1]*Dipartimento di Fisica, Università degli Studi di Milano, via Celoria 16, 20133 Milan, Italy*

[2]*Dipartimento di Scienze Farmacologiche e Biomolecolari, Università degli Studi di Milano, via Trentacoste 2, 20134 Milan, Italy*

[3]*Istituto di Nanoscienze – CNR, Modena, Italy*

ABSTRACT

Several studies suggest that the plasma membrane is composed of micro-domains of saturated lipids that segregate together to form lipid rafts. Lipid rafts have been operationally defined as cholesterol- and sphingolipid-enriched membrane micro-domains resistant to solubilisation by non-ionic detergents at low temperatures. Here we report a biophysical approach aimed at investigating lipid rafts of MDA-MB-231 human breast cancer cells by coupling an Atomic Force Microscopy (AFM) study to biochemical assays namely Western Blotting and High Performance Thin Layer Chromatography. Lipid rafts were purified by ultracentrifugation on discontinuous sucrose gradient using extraction with Triton X-100. Biochemical analyses proved that the fractions isolated at the 5% and 30% sucrose interface (fractions 5 and 6) have an higher content of cholesterol, sphingomyelin and flotillin-1 with respect to the other purified fractions. Tapping mode AFM imaging of fraction 5 showed membrane patches whose height corresponds to the one awaited for a single lipid bilayer as well as the presence of micro-domains with lateral dimensions in the order of a few hundreds of nanometers. In addition, an AFM study using specific antibodies suggests the presence, in these micro-domains, of a characteristic marker of lipid rafts, the protein flotillin-1.

KEYWORDS

lipid rafts, Atomic Force Microscopy, MDA-MB-231 cancer cells.

Corresponding author: Dr Francesco Orsini, Physics Dept., University of Milan, via Celoria 16, 20133 Milan, Italy. Phone: +39 0250315796; Fax: +39 0250315775; E-mail: francesco.orsini@unimi.it

*These authors contributed equally to this work.

1. INTRODUTION

Accumulating evidence indicates that cell membrane constituents might be not randomly distributed but rather organized in small lipid/protein domains enriched in sphingomyelin (SM) and cholesterol (CHOL), known as lipid rafts [1, 2]. Lipid rafts are small, heterogeneous, highly dynamic, sterol- and sphingolipid-enriched domains resistant to solubilisation by non-ionic detergents (traditionally Triton X-100) at low temperatures [3]. Moreover, lipid rafts are enriched in GPI-anchored proteins [4] and also contain several signaling proteins, including for instance the epidermal growth factor receptor (EGFR) [5]. Proof of the existence of lipid rafts is based largely on biochemical evidence even if the lipid raft hypothesis is still a contentious topic, with much of the scientific community divided. In particular, the inability to visualize lipid rafts directly in cell membranes, as well as a lack of understanding of some basic properties (e.g. size and lifetime), has led to controversy over their definition and existence.

To date, a large number of experimental results converge toward the idea that lateral domains enriched in SM and CHOL exist in native biological membranes. These micro-domains have been suggested to take part in various dynamic cellular processes such as membrane trafficking, signal transduction, and regulation of the activity of membrane proteins [1, 6, 7].

In model membranes, the coexistence of domains in liquid ordered and liquid disordered phases is widely accepted [8, 9]. Self-associative properties unique to sphingolipids and CHOL in vitro could facilitate selective lateral segregation in the membrane plane and serve as a basis for lipid sorting in vivo [1].

Studying lipid rafts is challenging since they are probably too small to be resolved by techniques such as optical and fluorescence microscopy. However, super resolution microscopy offers, in principle, the possibility to investigate samples with these size ranges. For example, stimulated-emission-depletion (STED) nanoscopy (10) provided direct evidence in live cells that certain lipids are transiently trapped in CHOL-assisted molecular complexes (11, 12, 13). These studies revealed that the extent of the areas in which the lipids dwell during trapping is about 20 nm in diameter (11). Photoactivated localization microscopy (PALM) is another powerful approach for investigating protein/lipid organization. Combining pair-correlation analysis with PALM provided a method to analyze complex patterns of protein organization across the plasma membrane demonstrating a distinct nanoscale organization of plasma membrane proteins with different membrane anchoring and lipid partitioning characteristics in COS-7 cells as well as dramatic changes in GPI-anchored protein arrangement under varying perturbations (14). Moreover, PALM imaging proved that CHOL- and sphingolipid-enriched micro-domains occupy different regions on

the plasma membrane with lateral dimensions in the order of an hundred of nanometers (15). Atomic Force Microscopy (AFM), providing nanometer spatial resolution and operating in physiological-like conditions without fixation, staining, or labelling, appears to be an useful tool to quantitatively perform a morpho-dimensional characterization of lipid rafts as well as of their protein content [16]. Moreover, thanks to its high signal-to-noise ratio, AFM allows to monitor function related structural conformational changes and to observe structural details of membrane proteins under physiological conditions, revealing information on the protein oligomeric state and on the supramolecular architecture of membrane protein complexes [17-19].

In this work we applied AFM, together with biochemical assays, namely Western Blotting (WB) and High Performance Thin Layer Chromatography (HP-TLC), to the study of lipid rafts of MDA-MB-231 human breast cancer cells. In particular, the different fractions, isolated in the purification process by ultracentrifugation on sucrose gradient, have been analysed with respect to their lipid content and morpho-dimensionally characterized. Interestingly, AFM imaging of the purified fractions with the richest CHOL and SM content, showed membrane micro-domains with lateral dimensions of a few hundreds of nanometers. Moreover, treating the samples with a specific antibody against the protein flotillin-1, an increase of the micro-domain surface area occurs thus suggesting the presence of flotillin-1, a lipid raft-associated protein [20], in the visualized membrane micro-domains.

2. MATERIALS AND METHODS

2.1 Cell line and culture conditions

Human breast cancer cell line MDA-MB-231 (ER-negative and over-expressing EGFR), derived from human mammary adenocarcinoma, were obtained from Italian National Cancer Research Institute cell bank. The MDA-MB-231 cell line was maintained in DMEM medium (Gibco-BRL, Life Technologies Italia srl, Italy) supplemented with 10% fetal bovine serum (FBS), 100 U/ml penicillin, 100 mg/ml streptomycin and 2 mM glutamine. Cells were grown at 37 °C in a 5% CO_2 atmosphere with 98% relative humidity.

2.2 Lipid raft isolation

Cells were seeded at 1.5 x 10^4 cells/cm^2 in DMEM medium. After 48 h, cells were harvested by scraping in phosphate-buffered saline containing 0.4 mM Na_3VO_4. Cells were centrifuged and lysed in ice-cold lysis buffer containing 1% Triton X-100 for 20 min. Lysates were disrupted by a tight-fitting Dounce homogenizer. The cell lysate was centrifuged at 1300g for 5 min at 4 °C, and the postnuclear supernatant (PNS) was transferred to an eppendorf tube. 1 ml of PNS was mixed

with 1 ml of ice-cold 85% w/v sucrose and then overlaid with 5.5 ml of 30% and 4 ml 5% w/v sucrose. Tubes were centrifuged at 200,000g for 17 h at 4 °C in a Ultracentrifuge (Beckman Coulter). Different fractions (1 ml/fraction) were collected sequentially from the top of the gradient (fraction 1) to the bottom (fraction 11). In order to confirm the purification of lipid rafts, the content of CHOL, SM and flotillin-1 was determined in each fraction by HP-TLC and WB.

2.3 Western blot analysis for flotillin-1

All fractions were separated by SDS-PAGE (10% polyacrylamide gel) and transferred onto a polyvinylidene difluoride (PVDF) membrane overnight then blocked in blocking buffer consisting of 5% (w/v) dried non-fat milk in Tris-buffered saline (T-TBS: 10 mM Tris/HCl, pH 7.5, 150 mM NaCl, 0.1% (v/v) Tween®20) at room temperature for 1 h. The blots were treated with anti-flotillin-1 primary antibodies diluted 1:200 in blocking buffer at room temperature for 2 h, washed with T-TBS and incubated with the proper secondary antibody in blocking buffer at room temperature for 1 h. The protein bands were visualized using enhanced chemiluminescence (ECL) reagents (PerkinElmer, USA).

2.4 Lipid composition analysis

Lipids were extracted from each fraction with three different chloroform/methanol mixtures (1/1, 1/2 and 2/1, v/v) and partitioned with the theoretical upper phase (TUP, chloroform/methanol/water, 47/48/1, by volume) and then with water. The organic phase was dried and then suspended in chloroform/methanol (2/1, v/v) for the analysis of CHOL and SM.

Free CHOL and SM were quantified by HP-TLC with hexane/ether/glacial acetic acid (90/10/1 by volume) and with chloroform/methanol/glacial acetic acid/water (60/45/4/2 by volume), respectively. CHOL was visualized with a solution of copper sulphate in phosphoric acid at 180 °C, while SM with anisaldehyde in acetic acid and sulphuric acid at 120 °C. CHOL and SM standards were spotted on the same plate.

2.5 Atomic Force Microscopy

A Nanoscope Multimode IIId (Bruker, Santa Barbara, CA, USA) AFM equipped with a 12 μm piezo scanner was used for the morpho-dimensional characterization of the different fractions of MDA-MB-231 cell membranes purified by ultracentrifugation.

Topography AFM images were collected in tapping mode [21] using the RMS amplitude of the cantilever as feedback signal operating in a saline liquid buffer. Rectangular nitrate silicon probes were used with nominal spring constant around 2.5 N/m (NT-MDT, Russia) and cantilever length of

120 μm. The cantilever resonance frequency was about 30 kHz. The RMS free amplitude of the cantilever was on the order of 15 nm and the relative set-point above 95% of the free amplitude. Images were recorded with a slow scan rate (below 1 Hz) and a resolution of 512x512 pixel per image was chosen.

2.6 Sample preparation for AFM imaging

Membrane samples were diluted 1:30 in distilled water. For AFM imaging 50 μl of diluted fractions, purified by ultracentrifugation, were floated on a freshly cleaved mica leaf, previously activated with 100 μl of adsorption buffer (150 mM KCl, 25 mM $MgCl_2$, 10 mM Tris/HCl, pH 7.5). After 10 min, the sample was gently rinsed three times with recording buffer (150 mM KCl, 10 mM Hepes/Tris, pH 7.5) to remove membrane fragments that have not been adsorbed to the support. Samples were visualized in tapping mode in recording buffer.

2.7 Antibody labelling

Membrane samples, adsorbed onto mica surface and prepared as above described, were incubated with rabbit polyclonal anti flotillin-1 antibodies raised against amino acids 324-427 of flotillin-1 (Santa Cruz Biotechnology, USA) diluted 1:4 in recording buffer as reported in literature [22] and imaged at different times (0, 30, 60 min). This protocol allowed direct comparison of the same membrane samples prior and after the antibody binding. For control experiments membrane samples, adsorbed onto mica surface and prepared as above described, were incubated with non specific antibodies, namely an anti-clathrin hc mouse monoclonal antibody raised against the N-terminus of clathrin heavy chain of human origin (Santa Cruz Biotechnology, USA) diluted 1:4 in recording buffer and imaged at different times (0, 30, 60 min).

3. RESULTS

In the present work, lipid rafts resistant to non-ionic detergent (Triton X-100) extraction were isolated from MDA-MB-231 human breast cancer cells by ultracentrifugation on discontinuous sucrose gradient as described in details in Materials and Methods. The presence of lipid rafts was verified detecting in all the 11 collected fractions the lipid raft-associated protein flotillin-1 [20] by SDS-PAGE assay and WB analysis. In figure 1 the distribution of flotillin-1 in the 11 fractions purified by ultracentrifugation is reported. In particular, the highest flotillin-1 content was found in the low-density fractions (fractions 5 and 6) corresponding to the 5% and 30% sucrose interface.

Moreover, the analysis of the distribution of some lipids highly present in lipid rafts, namely CHOL and phospholipids such as SM, carried out by HP-TLC assay confirmed the presence of these detergent-resistant membrane micro-domains in the 5 and 6 purified fractions. Figures 2a and 2b show the distribution of CHOL and SM content in all the 11 fractions purified by ultracentrifugation. As in the case of flotillin-1, fractions 5 and 6 have the richest content both of CHOL and SM thus suggesting a larger presence of lipid rafts in these samples.

In order to perform a morpho-dimensional characterization of lipid rafts, all the 11 fractions purified in the ultracentrifugation process were visualized by AFM.

In Figure 3, as an example, AFM topography images of some among the 11 fractions are reported. In particular, membrane patches with lateral sizes of a few microns and height of about 4 nm, as awaited for lipid bilayers, are clearly visible in the fractions 5 and 7. Moreover, the number of membrane patches decreases moving from fraction 5 to 7. AFM images of fraction 6 (not shown) are very similar to the fraction 5. The situation dramatically changes visualizing the other fractions, where only small membrane fragments with lateral dimensions of a few dozen of nanometers are visualized on the mica support (fractions from 1 to 4, 8 and 9). Fractions 10 and 11 show a continuous and homogeneous distribution of membrane fragments on the whole mica surface. It is worth noting that these fractions are recovered at the bottom of the tube exactly where the PNS is placed before the ultracentrifugation process.

Taken together, the biochemical analyses and AFM imaging indicate that lipid rafts are mainly present in the low-density fractions (fractions 5 and 6) corresponding to the 5% and 30% sucrose interface. For this reason a more detailed AFM investigation has been performed on these fractions. Samples prepared from fraction 5 showed membrane patches with micro-domains protruding from their surface as reported in Figure 4. In particular, different regions can be easily identified: the mica support (1), the membrane patch (2), two membrane micro-domains (3) and finally aggregates (white areas) which exhibit an height of a few dozen of nanometers.

The dimensional characterization of the structures observed in Figure 4 and obtained analysing several AFM topography images collected in tapping mode in buffer solution gave, for membrane patches, lateral sizes in the range of 1-3 μm while their thickness, on average, of about 4 nm suggests that lipid bilayers were visualized (see Figure 5). The lateral dimensions of the micro-domains visualized on the membrane patch surface were mainly in the range of 100-500 nm and always well under 1 μm. Moreover, these regions protrude by 1-2 nm from the surrounding membrane as shown in the height profile reported in Figure 5 (red arrows). The brighter areas visible on membrane patches could be identified as protein aggregates probably produced during the sample deposition process and induced by the interactions with the mica support.

Surface roughness of membrane patches (areas like the ones labelled 2 in Figure 4) as well as of the membrane micro-domains (areas like the ones labelled 3 in Figure 4), expressed as differences in the root-mean-square of the vertical Z dimension values within the examined areas, was calculated according to the following equation:

$$rms_{xy} = \sqrt{\sum_{x,y=1}^{N} \frac{(Z_{x,y} - Z_{average})^2}{N^2}}$$

where $Z_{average}$ is the average Z value within the examined area, $Z_{x,y}$ is the local Z value and N indicates the number of points within the area.

Rms surface roughness values were calculated as the mean of at least 15 measurements on 50x50 nm^2 square areas collected on the surface of membrane patches and membrane micro-domains observed in several AFM topography images. Errors were estimated as standard deviation. All the membrane micro-domains exhibited a similar surface corrugation while in comparison the membrane patch surface appears to be very smooth. In particular, rms surface roughness of 0.26 ± 0.03 nm (mean ± SD; n = 18) and of 0.11 ± 0.01 nm (mean ± SD; n = 15) were calculated for membrane micro-domains and for membrane patches respectively.

The micro-domains visualized on the membrane patch surface appear to be very interesting since their dimensions are in line with the range expected for lipid rafts as reported extensively in literature [23, 24]. For this reason we also performed a high resolution AFM imaging of these areas aiming at obtaining more detailed insights.

In particular, the AFM image obtained scanning an area of a few hundreds square nanometers and reported in Figure 6, shows a micro-domain protruding by about 1 nm from the membrane surface (red arrows). The micro-domain has a mean rms surface roughness of 0.25 nm, easily visible in the AFM image, while the surrounding membrane is very smooth with a mean rms surface roughness of only 0.10 nm. Moreover, the height profile points out some structural features on the micro-domain surface with heights lower than 1 nm and lateral sizes of a few nanometers thus suggesting the presence of proteins embedded in the micro-domain. Unfortunately these nanometer structures appear to be too soft and movable, under the AFM scanning tip, to collect better detailed images even applying very low forces.

In order to obtain both more information regarding the nature of the micro-domains visualized on the membrane patch surface and to identify the proteins observed in these areas, we carried out also a study using specific antibodies. In particular, membrane patches adsorbed onto the mica surface

were incubated with rabbit polyclonal antibodies raised against amino acids 324-427 of flotillin-1, a protein segment near the C-terminus and fully exposed in the cytoplasmic side of the plasma membrane. Anti flotillin-1 antibodies were diluted 1:4 while AFM scanning and images were collected at different times (0, 30, 60 min) allowing the direct comparison of the same membrane patches before and after antibody binding. After just 60 min incubation with the anti flotillin-1 antibodies, the micro-domains changed their appearance showing a surface area enlargement as clearly visible in Figure 7 thus indicating antibody binding.

To demonstrate specificity and get rid of possible physisorption phenomena, as control experiment non specific antibodies were used. In particular, membrane samples adsorbed onto the mica surface were incubated with antibodies raised against a non raft protein marker (clathrin hc) [25]. Mouse monoclonal anti clathrin hc antibodies raised against the N-terminus of clathrin heavy chain were diluted 1:4 in recording buffer and AFM images were collected. The shape and dimensions of the micro-domains visualized at different times (0, 30, 60 min) were comparable (not shown).

A more detailed quantitative analysis allowed to calculate that the surface area of the micro-domains protruding from the smooth lipid membrane increased by about 20% upon antibody binding so confirming the protein nature of the nanometer structures visualized on the micro-domain surface. We have estimated the increase of the surface area as follows. The contour line of a number of membrane patches as well as of micro-domains protruding from the membrane patch surface were marked before and after 60 min treatment with anti flotillin-1 antibody directly from several AFM images using the Image J 1.45 software (NIH, USA). The increase of the surface area was calculated as the percentage variation compared to the untreated sample measured in pixels. In particular we found a surface area increase of 20.7 ± 5.6% (mean ± SD; n = 11) and 8.3 ± 2.4% (mean ± SD; n = 10) for micro-domains and membrane patches respectively as shown in the histogram reported in Figure 8. The observed difference between the surface area increase of membrane patches and micro-domains caused by the antibody treatment was statistically significant (t-Student's test: $P < 0.01$). In the control experiment, the same analysis gave an increase of the surface area of 8.1 ± 1.6% (mean ± SD; n = 10) and 9.4 ± 2.5% (mean ± SD; n = 10) for micro-domains and membrane patches respectively (see Figure 8). The difference between the surface area increase of micro-domains, caused by the anti flotillin-1 antibody treatment, and of membrane patches and micro-domains in the control experiment was statistically significant (t-Student's test: $P < 0.01$) too.

It is worth noting that the surface area increase in the anti flotillin-1 experiment showed for membrane patches a normal distribution centered on about 8%, while for membrane micro-domains the surface area increase was distributed in two different ranges, 8-10% as for membrane patches

and the control experiment, and higher values around 24-27%. The following consideration could explain this behaviour. The sample preparation protocol for AFM imaging we used in the present work does not allow to select the orientation of the membrane patches visualized on the mica support. Since anti flotillin-1 antibody binds to the cytoplasmic side of the plasma membrane, a surface area increase of about 10% could be awaited for membrane micro-domains exposing the external face of the plasma membrane due to non specific physisorption phenomena. Consequently, the surface area increase of about 20%, calculated for the membrane micro-domains and induced by the anti flotillin-1 antibody binding, could be an underestimation of the real value.

Moreover, although the enlargement of the micro-domain surface area is the more evident effect visible in AFM images (see Figure 7), it is expected that antibody binding should also result in an increase of height and surface corrugation of the micro-domains [26].

The analysis of the height profiles derived from cross-sections perpendicular to the micro-domain long axis and obtained by AFM topography images collected before and after the anti flotillin-1 treatment made difficult to quantify a reliable difference even if the experimental data showed a slight increase of the micro-domain height and the height profiles exhibited a higher corrugation after the antibody binding. Quantitative information were obtained by the analysis of the rms surface roughness. In particular, the rms surface roughness of the membrane micro-domains, measured on 50x50 nm^2 square areas, increased from 0.25 ± 0.03 nm (mean ± SD; n = 11) to 0.34 ± 0.03 nm (mean ± SD; n = 11) after the antibody binding.

The experimental data pointing out the effect induced by the antibody specific binding suggest the presence of flotillin-1 in the membrane micro-domains. Moreover, the flotillin-1 recognition, a lipid raft-associated protein [20], and its high content in these membrane micro-domains strongly support the hypothesis that the areas visualized in the AFM images and protruding from the membrane patch surface could be identified as lipid rafts.

4. DISCUSSION AND CONCLUSIONS

Lipid rafts, small and highly dynamic micro-domains enriched in SM and CHOL located in the native biological membranes [1, 2], are suggested to play a significant role in many cellular processes such as membrane trafficking, signal transduction and regulation of membrane protein activity [1, 6, 7].

Many experimental tools have been used to identify lipid rafts and to clarify their physiological significance even if, till now, their existence is still a contentious topic. Along with specific antibodies for detecting raft proteins, bacterial toxins that target lipid components are often used as raft markers [27-29]. AFM has been shown to be a very useful technique to visualize and

quantitatively characterize the topology of biological membranes also in physiological-like conditions [17-19]. In the present study we applied tapping mode AFM imaging to investigate lipid rafts of MDA-MB-231 human breast cancer cells. In tapping mode AFM the tip, mounted at the end of a cantilever vibrating at its resonant frequency, is placed near the sample and taps the surface only at the end of each oscillation cycle. The cantilever amplitude is held constant by altering the vertical position of the scanner. The topography image is then computed from the changes in scanner vertical position. Because the tip only makes intermittent contact with the sample, the lateral forces applied to the surface during the scanning are reduced and so tapping mode AFM is a very efficient imaging mode to study soft samples such as biological macromolecules and bio-membranes. Morpho-dimensional AFM analysis was also coupled with WB and HP-TLC assays to obtain a biochemical characterization of the structures visualized in AFM images. Membrane patches of MDA-MB-231 cell resistant to Triton X-100 extraction were purified by ultracentrifugation on a discontinuous sucrose gradient. All the 11 isolated fractions were analysed with respect to their flotillin-1 content by SDS-PAGE and WB assays. Fractions 5 and 6 showed the highest levels of flotillin-1, a lipid raft associated protein [20], as reported in Figure 1. Moreover, HP-TLC analysis detected in the same purified fractions the highest content of CHOL and SM, lipids highly present in lipid rafts (see Figure 2). The biochemical data therefore confirm a larger presence of lipid rafts in the low-density fractions 5 and 6 corresponding to the 5% and 30% sucrose interface. In agreement with biochemical analyses, AFM imaging visualized large and planar membrane patches with lateral sizes of a few microns and an height of about 4-5 nm, as awaited for single lipid bilayers, only in the fractions with the richest content of flotillin-1, CHOL and SM (see Figure 3). Moreover, the number of the membrane patches decreases from fraction 5 to 7 as well as the flotillin-1, CHOL and SM content.

Classical preparation of lipid rafts uses 1% Triton X-100 to extract detergent resistant membranes which are then separated by ultracentrifugation on 5%-30% sucrose density gradient. Recently, different methods have been developed using a variety of other detergents or with detergent free techniques [30]. Some observations raised the hypothesis that treatment of cells with detergents may generate clusters of raft lipids and proteins that did not exist in the intact cells. Our data showed in fractions 5 and 6 the presence of membrane patches of 1-3 μm that may be formed through a mechanism of coalescence as a result of detergent treatment. Nevertheless recent data demonstrated that Triton X-100 does not induce domain formation or increase the fraction of the bilayer in the ordered state, although it does increase domain size by coalescing pre-existing domains [30]. Thus our observations are in agreement with this theory.

Interestingly high resolution AFM imaging of samples prepared from fraction 5 showed micro-domains protruding from the membrane patches by 1-2 nm and with lateral dimensions in the range of 100-500 nm in line with the range expected for lipid rafts [23, 24] as shown in Figures 4 and 5. In addition, while the surrounding membrane appears to be very smooth (rms surface roughness = 0.11 ± 0.01 nm; mean ± SD, n = 15), the micro-domain exhibits a surface corrugation (rms surface roughness = 0.26 ± 0.03 nm; mean ± SD, n = 18) with nanometer features on its surface which resemble proteins in both size and shape (see Figure 6).

The incubation of membrane patches with anti flotillin-1 antibody proved the protein nature of the structures visualized on the micro-domain surface as well as the presence of flotillin-1 among these proteins. In fact, as reported in Figure 7, just after 60 min of anti flotillin-1 antibody treatment the micro-domains changed their size and appearance showing an evident enlargement of the surface area. In particular the micro-domain surface area increased by about 20% while membrane patches showed an average increase of only about 8% (see Figure 8). The observed difference was statistically significant (t-Student's test: $P < 0.01$). Besides, membrane micro-domains exhibited a higher surface corrugation after the antibody binding and their rms surface roughness increased from 0.25 ± 0.03 nm (mean ± SD; n = 11) to 0.34 ± 0.03 nm (mean ± SD; n = 11).

On the contrary, control experiments carried out using anti clathrin hc, a non specific antibody raised against a non raft protein marker [25], showed an average increase of the surface area of about 8% for micro-domains as well as for membrane patches (see Figure 8). The increase of the membrane patch surface area, of the same order both in the anti flotillin-1 treated and control experiments, could be caused by re-aggregation processes of lipid aggregates not well adhered to the mica support.

Interestingly, the increase of the surface area of the membrane micro-domains induced by the anti flotillin-1 treatment showed values distributed in two different ranges, 8-10% and 24-27%. These differences can be justified taken in account that the sample preparation protocol for AFM imaging does not allow to select the orientation of the membrane patches on the mica support. Since anti flotillin-1 binds to the cytoplasmic side of the plasma membrane, the 8-10% surface area increase could be induced by non specific physisorption phenomena on micro-domains exposing the external face of the membrane. As a result the increase of the micro-domain surface area of about 20% induced by the anti flotillin-1 antibody binding could be an underestimation of the real value.

4.1 Concluding remarks

Taken together the biochemical data as well as the flotillin-1 recognition and its high content in the membrane micro-domains, strongly indicate that the nanometer areas protruding from the

membrane patch surface and visualized in AFM images are lipid rafts. Moreover, our results are in favourable agreement with data reported in literature and obtained using different experimental approaches [2]. We believe that further applications of AFM imaging to lipid raft topic in both healthy and pathological native biological membranes coupled with a detailed biochemical investigation could contribute to better understanding some basic properties and molecular mechanisms of this important biological phenomenon.

ACKNOWLEDGEMENTS

The authors thank the Banca del Monte di Lombardia Foundation for its support for AFM instrumentation purchasing. This work was supported by ASI (MoMa) grant to A.M.R.

REFERENCES

[1] K. Simons and E. Ikonen, Functional rafts in cell membranes, Nature 387 (1997) 569–572.

[2] K. Simons and W.L. Vaz, Model systems, lipid rafts, and cell membranes, Annu. Rev. Biophys. Biomol. Struct. 33 (2004) 269–295.

[3] D.A. Brown, E. London, Functions of lipid rafts in biological membranes, Annu Rev Cell Dev Biol. 14 (1998) 111–36.

[4] A.S. Shaw, Lipid rafts: now you see them, now you don't, Nat. Immunol. 7 (2006) 1139–42.

[5] L.J. Foster, C.L. De Hoog, M. Mann, Unbiased quantitative proteomics of lipid rafts reveals high specificity for signaling factors, Proc. Natl. Acad. Sci. USA 100 (2003) 5813–8.

[6] S. Mayor and M. Rao, Rafts: scale-dependent, active lipid organization at the cell surface, Traffic 5 (2004) 231–240.

[7] M. Edidin, The state of lipid rafts: From model membranes to cells, Annu Rev Biophys Biomol Struct 32 (2003) 257–283.

[8] E. London, How principles of domain formation in model membranes may explain ambiguities concerning lipid raft formation in cells, Biochim. Biophys. Acta 1746 (2005) 203–220.

[9] P.F.F. Almeida, A. Pokorny, A. Hinderliter, Thermodynamics of membrane domains, Biochim. Biophys. Acta 1720 (2005) 1–13.

[10] S.W. Hell, J. Wichmann, Breaking the diffraction resolution limit by stimulated emission: Stimulated emission depletion microscopy, Opt. Lett. 19 (1994) 780–782.

[11] C. Eggeling, C. Ringemann, R. Medda, G. Schwarzmann, K. Sandhoff, S. Polyakova, V.N. Belov, B. Hein, C. von Middendorff, A. Schonle and S.W. Hell, Direct observation of the nanoscale dynamics of membrane lipids in a living cell, Nature 457 (2009) 1159–1163.

[12] C. Ringemann, B. Harke, C. von Middendorff, R. Medda, A. Honigmann, R. Wagner, M. Leutenegger, A. Schonle, S.W. Hell and C. Eggeling, Exploring single-molecule dynamics with fluorescence nanoscopy, New J. Phys. 11 (2009) 103054.

[13] S.J. Sahl, M. Leutenegger, M. Hilbert, S.W. Hell and C. Eggeling, Fast molecular tracking maps nanoscale dynamics of plasma membrane lipids, Proc. Natl. Acad. Sci. USA 107 (2010) 6829-6834.

[14] P. Sengupta, T. Jovanovic-Talisman, D. Skoko, M. Renz, S.L Veatch, J. Lippincott-Schwartz, Probing protein heterogeneity in the plasma membrane using PALM and pair correlation analysis, Nature Methods 8 (2011) 969-975.

[15] H. Mizuno, M. Abe, P. Dedecker, A. Makino, S. Rocha, Y. Ohno-Iwashita, J. Hofkens, T. Kobayashi, A. Miyawaki, Fluorescent probes for superresolution imaging of lipid domains on the plasma membrane, Chemical Science 2 (2011) 1548-1553.

[16] C.R. Anderton, K. Lou, P.K. Weber, I.D. Hutcheon, M.L. Kraft, Correlated AFM and NanoSIMS imaging to probe cholesterol-induced changes in phase behaviour and non-ideal mixing in ternary lipid membranes, Biochim. Biophys. Acta 1808 (2011) 307-315.

[17] B.W. Hoogenboom, K. Suda, A. Engel, D. Fotiadis, Supramolecular assemblies of the voltage-dependent anion channel in the native membrane, J. Mol. Biol. 370 (2007) 246–255.

[18] D.J. Muller, A. Engel, Conformational changes, flexibilities and intramolecular forces observed on individual proteins using AFM, RIKEN Rev. 36 (2001) 29–31.

[19] S. Scheuring, AFM studies of the supramolecular assembly of bacterial photosynthetic core-complexes, Curr. Opin. Chem. Biol. 10 (2006) 387–393.

[20] L.J. Pike, Lipid rafts: bringing order to chaos, J. Lipid Research 44 (2003) 655-667.

[21] P.K. Hansma, J.P. Cleveland, M. Radmacher, D.A. Walters, P.E. Hillner, M. Bezanilla, M. Fritz, D. Vie, H.G. Hansma, C.B. Prater, Tapping mode atomic-force microscopy in liquids, Appl. Phys. Lett. 64 (1994) 1738–1740.

[22] N. Buzhynskyy, C. Salesse and S. Scheuring, Rhodopsin is spatially heterogeneously distributed in rod outer segment disk membranes. J. Mol. Recognit, 24 (2011) 483–489.

[23] G.J. Schütz, G. Kada, V.Ph. Pastushenko and H. Schindler, Properties of lipid microdomains in a muscle cell membrane visualized by single molecule microscopy, The EMBO J. 19 (2000) 892-901.

[24] D. Lingwood and K. Simons, Lipid Rafts as a Membrane-Organizing Principle, Science 327 (2010) 46-50.

[25] N. Fabelo, V. Martin, G. Santpere, R. Marin, L. Torrent and M. Diaz, Severe alterations in lipid composition of frontal cortex lipid rafts from Parkinson's disease and incidental Parkinson's disease, Molecular Medicine 17 (2011) 1107–1118.

[26] D.J. Muller, C.A. Schoenenberger, G. Buldt and A. Engel, Immuno-Atomic Force Microscopy of Purple Membrane, Biophysical J. 70 (1996) 1796-1802.

[27] R.G. Parton, Ultrastructural localization of gangliosides; GM1 is concentrated in caveolae, J. Histochem. Cytochem. 42 (1994) 155–166.

[28] M. Fivaz, L. Abrami, F.G. van der Goot, Landing on lipid rafts, Trends Cell Biol. 9 (1999) 212–213.

[29] A. Yamaji, Y. Sekizawa, K. Emoto, H. Sakuraba, K. Inoue, H. Kobayashi, M. Umeda, Lysenin, a novel sphingomyelin-specific binding protein, J. Biol. Chem. 273 (1998) 5300–5306.

[30] P. Pathak, E. London, Measurement of lipid nanodomain (raft) formation and size in sphingomyelin/POPC/cholesterol vesicles shows TX-100 and transmembrane helices increase domain size by coalescing preexisting nanodomains but do not induce domain formation, Biophysical J. 101 (2011) 2417-2425.

FIGURE CAPTIONS

Figure 1.

Distribution of flotillin-1 in Triton X-100 isolated MDA-MB-231 human breast cancer cell membranes. Triton X-100 lysates of cell cultures were purified and fractionated by sucrose gradient ultracentrifugation. Equal volumes of each fraction were analysed by Western Blotting with antibodies to flotillin-1 protein. Fractions 5 and 6 have the highest flotillin-1 content.

Figure 2.

*Distribution of CHOL (**a**) and SM (**b**) content in Triton X-100 isolated MDA-MB-231 human breast cancer cell membranes. Triton X-100 lysates of cell cultures were purified and fractionated by sucrose gradient ultracentrifugation. Equal volumes of each fraction were analysed by HP-TLC. Fractions 5 and 6 have the highest content of CHOL and SM.*

Figure 3.

AFM topography images of some isolated fractions. Purified membranes were diluted 1:30 in distilled water and 50 μl of the suspension placed on a mica support. AFM images were collected in liquid buffer in tapping mode. Different situations were visualized: membrane patches with lateral sizes of a few microns and height of 4 nm (fractions from 5 to 7), small membrane fragments (fractions from 1 to 4, 8 and 9) and an homogeneous distribution of membrane fragments on the whole support (fractions 10 and 11). For all the images: scan area = 10x10 μm^2; z range (from darkest to lightest) = 20 nm; scale bar = 1 μm.

Figure 4.

AFM topography image of a membrane sample prepared from fraction 5 collected in liquid buffer in tapping mode. Different regions are visualized: the mica support (1), a membrane patch (2), two micro-domains protruding from the membrane surface (3) and higher aggregates (white areas).
Scan area = 1.5x1.5 μm^2; z range (from darkest to lightest) = 15 nm.

Figure 5.

*(**left**) AFM topography image of a membrane sample prepared from fraction 5 and collected in liquid buffer in tapping mode. The image shows a membrane patch 4 nm thick (green arrows) with two micro-domains and some protein aggregates (brighter areas). (**right**) Height profile corresponding to the black line drawn in AFM image. The micro-domain protrudes by 2 nm from the membrane surface (red arrows). Scan area = 1.6x1.6 μm^2; z range (from darkest to lightest) = 20 nm.*

Figure 6.

*(**left**) High resolution AFM topography image of a membrane sample prepared from fraction 5 and collected in liquid buffer in tapping mode. The image shows a micro-domain (1) which protrudes by about 1 nm from the surface (2) of the membrane patch (red arrows). The micro-domain has a surface roughness while the surrounding membrane is very smooth. (**right**) Height profile corresponding to the black line drawn in AFM image. Nanometer features are visible on the micro-domain surface comparable for dimensions with proteins. Scan area = 200x200 nm^2; z range (from darkest to lightest) = 2 nm.*

Figure 7.

*AFM topography images of membrane samples prepared from fraction 5 and collected in liquid buffer in tapping mode. Untreated membrane patches (**a**) were incubated with anti flotillin-1 antibody (1:4 in adsorption buffer) for different times (0, 30, 60 min). Just after 60 min of treatment (**b**) the surface area of micro-domains protruding from the membrane patches clearly increases (see circled areas) thus suggesting the presence of flotillin-1 proteins. Scan area = 5x5 μm^2; z range (from darkest to lightest) = 25 nm.*

Figure 8.

Histogram of the surface area increase for membrane patches, 8.3 ± 2.4% (mean ± SD; n = 10), and micro-domains, 20.7 ± 5.6% (mean ± SD; n = 11), after 60 min anti flotillin-1 antibody incubation (gray bars) and of the surface area increase for membrane patches, 9.4 ± 2.5% (mean ± SD; n = 10), and micro-domains, 8.1 ± 1.6% (mean ± SD; n = 10), in the control experiment after 60 min anti clathrin hc antibody incubation (white bars). The observed difference among the surface area increase of the micro-domains, induced by the anti flotillin-1 treatment, and of membrane patches both in the anti flotillin-1 treated and control experiment as well as of the micro-domains in the control experiment is statistically significant (t-Student's test: $P < 0.01$).

Atomic force microscopy imaging of lipid rafts of human breast cancer cells

[1]F.Orsini*, [2]A.Cremona*, [1]P.Arosio, [2]P.A.Corsetto, [2]G. Montorfano, [1,3]A.Lascialfari, [2]A.M.Rizzo

[1]*Dipartimento di Fisica, Università degli Studi di Milano, via Celoria 16, 20133 Milan, Italy*

[2]*Dipartimento di Scienze Farmacologiche e Biomolecolari, Università degli Studi di Milano, via Trentacoste 2, 20134 Milan, Italy*

[3]*Istituto di Nanoscienze – CNR, Modena, Italy*

ABSTRACT

Several ~~Recent~~ studies suggest that the plasma membrane is composed of micro-domains of saturated lipids that segregate together to form lipid rafts. Lipid rafts have been operationally defined as cholesterol- and sphingolipid-enriched membrane micro-domains resistant to solubilisation by non-ionic detergents at low temperatures. Here we report a biophysical approach aimed at investigating lipid rafts of MDA-MB-231 human breast cancer cells by coupling an Atomic Force Microscopy (AFM) study to biochemical assays namely Western Blotting and High Performance Thin Layer Chromatography. Lipid rafts were purified by ultracentrifugation on discontinuous sucrose gradient using extraction with Triton X-100. Biochemical analyses proved that the fractions isolated at the 5% and 30% sucrose interface (fractions 5 and 6) have an higher content of cholesterol, sphingomyelin and flotillin-1 with respect to the other purified fractions. Tapping mode AFM imaging of fraction 5 showed membrane patches whose height corresponds to the one awaited for a single lipid bilayer as well as the presence of micro-domains with lateral dimensions in the order of a few hundreds of nanometers. In addition, an AFM study using specific antibodies suggests the presence, in these micro-domains, of a characteristic marker of lipid rafts, the protein flotillin-1.

KEYWORDS

lipid rafts, Atomic Force Microscopy, MDA-MB-231 cancer cells.

Corresponding author: Dr Francesco Orsini, Physics Dept., University of Milan, via Celoria 16, 20133 Milan, Italy. Phone: +39 0250315796; Fax: +39 0250315775; E-mail: francesco.orsini@unimi.it

*These authors contributed equally to this work.

1. INTRODUTION

Accumulating evidence indicates that cell membrane constituents might be not randomly distributed but rather organized ~~Recent findings in membrane biology suggest that cell membrane constituents might be organized~~ in small lipid/protein domains enriched in sphingomyelin (SM) and cholesterol (CHOL), known as lipid rafts [1, 2]. Lipid rafts are small, heterogeneous, highly dynamic, sterol- and sphingolipid-enriched domains resistant to solubilisation by non-ionic detergents (traditionally Triton X-100) at low temperatures [3]. Moreover, lipid rafts are enriched in GPI-anchored proteins [4] and also contain several signaling proteins, including for instance the epidermal growth factor receptor (EGFR) [5]. Proof of the existence of lipid rafts is based largely on biochemical evidence even if the lipid raft hypothesis is still a contentious topic, with much of the scientific community divided. In particular, the inability to visualize lipid rafts directly in cell membranes, as well as a lack of understanding of some basic properties (e.g. size and lifetime), has led to controversy over their definition and existence.

To date, a large number of experimental results converge toward the idea that lateral domains enriched in SM and CHOL exist in native biological membranes. These micro-domains have been suggested to take part in various dynamic cellular processes such as membrane trafficking, signal transduction, and regulation of the activity of membrane proteins [1, 6, 7].

In model membranes, the coexistence of domains in liquid ordered and liquid disordered phases is widely accepted [8, 9]. Self-associative properties unique to sphingolipids and CHOL in vitro could facilitate selective lateral segregation in the membrane plane and serve as a basis for lipid sorting in vivo [1]. ~~Direct evidence of lipid rafts in vivo is mainly based on monitoring the motions of membrane proteins [2] or on differential partitioning of fluorescent probes in membrane environments [10].~~

Studying lipid rafts is challenging since they ~~with dimensions of a few hundreds nanometers,~~ are probably too small to be resolved by techniques such as optical and fluorescence microscopy. ~~High~~ However, super resolution microscopy offers, in principle, the possibility to investigate samples with these size ranges. ~~For example, Transmission Electron Microscope can visualize a 5-nanometer-thick cell membrane but it requires an invasive sample preparation (drying, staining and ultra-high vacuum).~~ For example, stimulated-emission-depletion (STED) nanoscopy (10) provided direct evidence in live cells that certain lipids are transiently trapped in CHOL-assisted molecular complexes (11, 12, 13). These studies revealed that the extent of the areas in which the lipids dwell during trapping is about 20 nm in diameter (11). Photoactivated localization microscopy (PALM) is another powerful approach for investigating protein/lipid organization. Combining pair-

correlation analysis with PALM provided a method to analyze complex patterns of protein organization across the plasma membrane demonstrating a distinct nanoscale organization of plasma membrane proteins with different membrane anchoring and lipid partitioning characteristics in COS-7 cells as well as dramatic changes in GPI-anchored protein arrangement under varying perturbations (14). Moreover, PALM imaging proved that CHOL- and sphingolipid-enriched micro-domains occupy different regions on the plasma membrane with lateral dimensions in the order of an hundred of nanometers (15). ~~On the contrary,~~ Atomic Force Microscopy (AFM), providing nanometer spatial resolution and operating in physiological-like conditions without fixation, staining, or labelling, appears to be an useful tool to quantitatively perform a morpho-dimensional characterization of lipid rafts as well as of their protein content [16]. Moreover, thanks to its high signal-to-noise ratio, AFM allows to monitor function related structural conformational changes and to observe structural details of membrane proteins under physiological conditions, revealing information on the protein oligomeric state and on the supramolecular architecture of membrane protein complexes [17-19].

In this work we applied AFM, together with biochemical assays, namely Western Blotting (WB) and High Performance Thin Layer Chromatography (HP-TLC), to the study of lipid rafts of MDA-MB-231 human breast cancer cells. In particular, the different fractions, isolated in the purification process by ultracentrifugation on sucrose gradient, have been analysed with respect to their lipid content and morpho-dimensionally characterized. Interestingly, AFM imaging of the purified fractions with the richest CHOL and SM content, showed membrane micro-domains with lateral dimensions of a few hundreds of nanometers. Moreover, treating the samples with a specific antibody against the protein flotillin-1, an increase of the micro-domain surface area occurs thus suggesting the presence of flotillin-1, a lipid raft-associated protein [20], in the visualized membrane micro-domains.

2. MATERIALS AND METHODS

2.1 Cell line and culture conditions

Human breast cancer cell line MDA-MB-231 (ER-negative and over-expressing EGFR), derived from human mammary adenocarcinoma, were obtained from Italian National Cancer Research Institute cell bank. The MDA-MB-231 cell line was maintained in DMEM medium (Gibco-BRL, Life Technologies Italia srl, Italy) supplemented with 10% fetal bovine serum (FBS), 100 U/ml penicillin, 100 mg/ml streptomycin and 2 mM glutamine. Cells were grown at 37 °C in a 5% CO_2 atmosphere with 98% relative humidity.

2.2 Lipid raft isolation

Cells were seeded at 1.5 x 10^4 cells/cm^2 in DMEM medium. After 48 h, cells were harvested by scraping in phosphate-buffered saline containing 0.4 mM Na_3VO_4. Cells were centrifuged and lysed in ice-cold lysis buffer containing 1% Triton X-100 for 20 min. Lysates were disrupted by a tight-fitting Dounce homogenizer. The cell lysate was centrifuged at 1300g for 5 min at 4 °C, and the postnuclear supernatant (PNS) was transferred to an eppendorf tube. 1 ml of PNS was mixed with 1 ml of ice-cold 85% w/v sucrose and then overlaid with 5.5 ml of 30% and 4 ml 5% w/v sucrose. Tubes were centrifuged at 200,000g for 17 h at 4 °C in a Ultracentrifuge (Beckman Coulter). Different fractions (1 ml/fraction) were collected sequentially from the top of the gradient (fraction 1) to the bottom (fraction 11). In order to confirm the purification of lipid rafts, the content of CHOL, SM and flotillin-1 was determined in each fraction by HP-TLC and WB.

2.3 Western blot analysis for flotillin-1

All fractions were separated by SDS-PAGE (10% polyacrylamide gel) and transferred onto a polyvinylidene difluoride (PVDF) membrane overnight then blocked in blocking buffer consisting of 5% (w/v) dried non-fat milk in Tris-buffered saline (T-TBS: 10 mM Tris/HCl, pH 7.5, 150 mM NaCl, 0.1% (v/v) Tween®20) at room temperature for 1 h. The blots were treated with anti-flotillin-1 primary antibodies diluted 1:200 in blocking buffer at room temperature for 2 h, washed with T-TBS and incubated with the proper secondary antibody in blocking buffer at room temperature for 1 h. The protein bands were visualized using enhanced chemiluminescence (ECL) reagents (PerkinElmer, USA).

2.4 Lipid composition analysis

Lipids were extracted from each fraction with three different chloroform/methanol mixtures (1/1, 1/2 and 2/1, v/v) and partitioned with the theoretical upper phase (TUP, chloroform/methanol/water, 47/48/1, by volume) and then with water. The organic phase was dried and then suspended in chloroform/methanol (2/1, v/v) for the analysis of CHOL and SM.

Free CHOL and SM were quantified by HP-TLC with hexane/ether/glacial acetic acid (90/10/1 by volume) and with chloroform/methanol/glacial acetic acid/water (60/45/4/2 by volume), respectively. CHOL was visualized with a solution of copper sulphate in phosphoric acid at 180 °C, while SM with anisaldehyde in acetic acid and sulphuric acid at 120 °C. CHOL and SM standards were spotted on the same plate.

2.5 Atomic Force Microscopy

A Nanoscope Multimode IIId (Bruker, Santa Barbara, CA, USA) AFM equipped with a 12 μm piezo scanner was used for the morpho-dimensional characterization of the different fractions of MDA-MB-231 cell membranes purified by ultracentrifugation.

Topography AFM images were collected in tapping mode [21] using the RMS amplitude of the cantilever as feedback signal operating in a saline liquid buffer. Rectangular nitrate silicon probes were used with nominal spring constant around 2.5 N/m (NT-MDT, Russia) and cantilever length of 120 μm. The cantilever resonance frequency was about 30 kHz. The RMS free amplitude of the cantilever was on the order of 15 nm and the relative set-point above 95% of the free amplitude. Images were recorded with a slow scan rate (below 1 Hz) and a resolution of 512x512 pixel per image was chosen.

2.6 Sample preparation for AFM imaging

Membrane samples were diluted 1:30 in distilled water. For AFM imaging 50 μl of diluted fractions, purified by ultracentrifugation, were floated on a freshly cleaved mica leaf, previously activated with 100 μl of adsorption buffer (150 mM KCl, 25 mM $MgCl_2$, 10 mM Tris/HCl, pH 7.5). After 10 min, the sample was gently rinsed three times with recording buffer (150 mM KCl, 10 mM Hepes/Tris, pH 7.5) to remove membrane fragments that have not been adsorbed to the support. Samples were visualized in tapping mode in recording buffer.

2.7 Antibody labelling ~~of flotillin-1~~

Membrane samples, adsorbed onto mica surface and prepared as above described, were incubated with rabbit polyclonal anti flotillin-1 antibodies raised against amino acids 324-427 of flotillin-1 (Santa Cruz Biotechnology, USA) diluted 1:4 in recording buffer as reported in literature [22] and imaged at different times (0, 30, 60 min). This protocol allowed direct comparison of the same membrane samples prior and after the antibody binding. ~~For control experiments 70 μL of recording buffer were poured on the membrane samples and AFM images were collected at different times (0, 30, 60 min).~~ For control experiments membrane samples, adsorbed onto mica surface and prepared as above described, were incubated with non specific antibodies, namely an anti-clathrin hc mouse monoclonal antibody raised against the N-terminus of clathrin heavy chain of human origin (Santa Cruz Biotechnology, USA) diluted 1:4 in recording buffer and imaged at different times (0, 30, 60 min).

3. RESULTS

In the present work, lipid rafts resistant to non-ionic detergent (Triton X-100) extraction were isolated from MDA-MB-231 human breast cancer cells by ultracentrifugation on discontinuous sucrose gradient as described in details in Materials and Methods. The presence of lipid rafts was verified detecting in all the 11 collected fractions the lipid raft-associated protein flotillin-1 [20] by SDS-PAGE assay and WB analysis. In figure 1 the distribution of flotillin-1 in the 11 fractions purified by ultracentrifugation is reported. In particular, the highest flotillin-1 content was found in the low-density fractions (fractions 5 and 6) corresponding to the 5% and 30% sucrose interface.

Moreover, the analysis of the distribution of some lipids highly present in lipid rafts, namely CHOL and phospholipids such as SM, carried out by HP-TLC assay confirmed the presence of these detergent-resistant membrane micro-domains in the 5 and 6 purified fractions. Figures 2a and 2b show the distribution of CHOL and SM content in all the 11 fractions purified by ultracentrifugation. As in the case of flotillin-1, fractions 5 and 6 have the richest content both of CHOL and SM thus suggesting a larger presence of lipid rafts in these samples.

In order to perform a morpho-dimensional characterization of lipid rafts, all the 11 fractions purified in the ultracentrifugation process were visualized by AFM. ~~This microscopy technique offers the possibility to observe biological specimens, such as cell membranes, with nanometer resolution in buffer solution without the need to preliminary treatments as sample fixation, staining or labelling. Thus, measurements can be made under near-native conditions in an aqueous environment.~~

In Figure 3, as an example, AFM topography images of some among the 11 fractions are reported. In particular, membrane patches with lateral sizes of a few microns and height of about 4 nm, as awaited for lipid bilayers, are clearly visible in the fractions 5 and 7. Moreover, the number of membrane patches decreases moving from fraction 5 to 7. AFM images of fraction 6 (not shown) are very similar to the fraction 5. The situation dramatically changes visualizing the other fractions, where only small membrane fragments with lateral dimensions of a few dozen of nanometers are visualized on the mica support (fractions from 1 to 4, 8 and 9). Fractions 10 and 11 show a continuous and homogeneous distribution of membrane fragments on the whole mica surface. It is worth noting that these fractions are recovered at the bottom of the tube exactly where the PNS is placed before the ultracentrifugation process.

Taken together, the biochemical analyses and AFM imaging indicate that lipid rafts are mainly present in the low-density fractions (fractions 5 and 6) corresponding to the 5% and 30% sucrose interface. For this reason a more detailed AFM investigation has been performed on these fractions.

Samples prepared from fraction 5 showed membrane patches with micro-domains protruding from their surface as reported in Figure 4. In particular, different regions can be easily identified: the mica support (1), the membrane patch (2), two membrane micro-domains (3) and finally aggregates (white areas) which exhibit an height of a few dozen of nanometers.

The dimensional characterization of the structures observed in Figure 4 and obtained analysing several AFM topography images collected in tapping mode in buffer solution gave, for membrane patches, lateral sizes in the range of 1-3 µm while their thickness, on average, of about 4 nm suggests that lipid bilayers were visualized (see Figure 5). The lateral dimensions of the micro-domains visualized on the membrane patch surface were mainly in the range of 100-500 nm and always well under 1 µm. Moreover, these regions protrude by 1-2 nm from the surrounding membrane as shown in the height profile reported in Figure 5 (red arrows). The brighter areas visible on membrane patches could be identified as protein aggregates probably produced during the sample deposition process and induced by the interactions with the mica support.

Surface roughness of membrane patches (areas like the ones labelled 2 in Figure 4) as well as of the membrane micro-domains (areas like the ones labelled 3 in Figure 4), expressed as differences in the root-mean-square of the vertical Z dimension values within the examined areas, was calculated according to the following equation:

$$rms_{xy} = \sqrt{\sum_{x,y=1}^{N} \frac{(Z_{x,y} - Z_{average})^2}{N^2}}$$

where $Z_{average}$ is the average Z value within the examined area, $Z_{x,y}$ is the local Z value and N indicates the number of points within the area.

Rms surface roughness values were calculated as the mean of at least 15 measurements on 50x50 nm^2 square areas collected on the surface of membrane patches and membrane micro-domains observed in several AFM topography images. Errors were estimated as standard deviation. All the membrane micro-domains exhibited a similar surface corrugation while in comparison the membrane patch surface appears to be very smooth. In particular, rms surface roughness of 0.26 ± 0.03 nm (mean ± SD; n = 18) and of 0.11 ± 0.01 nm (mean ± SD; n = 15) were calculated for membrane micro-domains and for membrane patches respectively.

The micro-domains visualized on the membrane patch surface appear to be very interesting since their dimensions are in line with the range expected for lipid rafts as reported extensively in

literature [23, 24]. For this reason we also performed a high resolution AFM imaging of these areas aiming at obtaining more detailed insights.

In particular, the AFM image obtained scanning an area of a few hundreds square nanometers and reported in Figure 6, shows a micro-domain protruding by about 1 nm from the membrane surface (red arrows). The micro-domain has a mean rms surface roughness ~~(white spots)~~ of 0.25 nm, easily visible in the AFM image, while the surrounding membrane is ~~appears to be~~ very smooth with a mean rms surface roughness of only 0.10 nm. Moreover, the height profile points out some structural features on the micro-domain surface with heights lower than 1 nm and lateral sizes of a few nanometers thus suggesting the presence of proteins embedded in the micro-domain. Unfortunately these nanometer structures appear to be too soft and movable, under the AFM scanning tip, to collect better detailed images even applying very low forces.

In order to obtain both more information regarding the nature of the micro-domains visualized on the membrane patch surface and to identify the proteins observed in these areas, we carried out also a study using specific antibodies. In particular, membrane patches adsorbed onto the mica surface were incubated with ~~anti-flotillin-1 antibody,~~ rabbit polyclonal antibodies raised against amino acids 324-427 of flotillin-1, a protein segment near the C-terminus and fully exposed in the cytoplasmic side of the plasma membrane. ~~a polyclonal antibody against the N-terminus of flotillin-1,~~ Anti flotillin-1 antibodies were diluted 1:4 while AFM scanning and images were collected at different times (0, 30, 60 min) allowing the direct comparison of the same membrane patches before and after antibody binding. After just 60 min incubation with the anti flotillin-1 antibodies, the micro-domains changed their appearance showing a surface area enlargement as clearly visible in Figure 7 thus indicating antibody binding. ~~As a control, 70 µL of recording buffer were poured on membrane patches and AFM images were collected. The shape and dimensions of the micro-domains visualized at different times (0, 30, 60 min) were comparable (not shown).~~

To demonstrate specificity and get rid of possible physisorption phenomena, as control experiment non specific antibodies were used. In particular, membrane samples adsorbed onto the mica surface were incubated with antibodies raised against a non raft protein marker (clathrin hc) [25]. Mouse monoclonal anti clathrin hc antibodies raised against the N-terminus of clathrin heavy chain were diluted 1:4 in recording buffer and AFM images were collected. The shape and dimensions of the micro-domains visualized at different times (0, 30, 60 min) were comparable (not shown).

A more detailed quantitative analysis allowed to calculate that the surface area of the micro-domains protruding from the smooth lipid membrane increased by about 20% upon antibody binding so confirming the protein nature of the nanometer structures visualized on the micro-domain surface. We have estimated the increase of the surface area as follows. The contour line of a

number of membrane patches as well as of micro-domains protruding from the membrane patch surface were marked before and after 60 min treatment with anti flotillin-1 antibody directly from several AFM images using the Image J 1.45 software (NIH, USA). The increase of the surface area was calculated as the percentage variation compared to the untreated sample measured in pixels. In particular we found a surface area increase of ~~17.8 ± 6.1% (mean ± SD; n = 12)~~ 20.7 ± 5.6% (mean ± SD; n = 11) and ~~7.9 ± 1.5% (mean ± SD; n = 10)~~ 8.3 ± 2.4% (mean ± SD; n = 10) for micro-domains and membrane patches respectively as shown in the histogram reported in Figure 8. The observed difference between the surface area increase of membrane patches and micro-domains caused by the antibody treatment was statistically significant (t-Student's test: $P < 0.01$). In the control experiment, the same analysis gave an increase of the surface area of ~~6.7 ± 1.7% (mean ± SD; n = 10)~~ 8.1 ± 1.6% (mean ± SD; n = 10) and ~~8.8 ± 1.9% (mean ± SD; n = 10)~~ 9.4 ± 2.5% (mean ± SD; n = 10) for micro-domains and membrane patches respectively (see Figure 8). The difference between the surface area increase of micro-domains, caused by the anti flotillin-1 antibody treatment, and of membrane patches and micro-domains in the control experiment was statistically significant (t-Student's test: $P < 0.01$) too.

It is worth noting that the surface area increase in the anti flotillin-1 experiment showed for membrane patches a normal distribution centered on about 8%, while for membrane micro-domains the surface area increase was distributed in two different ranges, 8-10% as for membrane patches and the control experiment, and higher values around 24-27%. The following consideration could explain this behaviour. The sample preparation protocol for AFM imaging we used in the present work does not allow to select the orientation of the membrane patches visualized on the mica support. Since anti flotillin-1 antibody binds to the cytoplasmic side of the plasma membrane, a surface area increase of about 10% could be awaited for membrane micro-domains exposing the external face of the plasma membrane due to non specific physisorption phenomena. Consequently, the surface area increase of about 20%, calculated for the membrane micro-domains and induced by the anti flotillin-1 antibody binding, could be an underestimation of the real value.

Moreover, although the enlargement of the micro-domain surface area is the more evident effect visible in AFM images (see Figure 7), it is expected that antibody binding should also result in an increase of height and surface corrugation of the micro-domains [26].

The analysis of the height profiles derived from cross-sections perpendicular to the micro-domain long axis and obtained by AFM topography images collected before and after the anti flotillin-1 treatment made difficult to quantify a reliable difference even if the experimental data showed a slight increase of the micro-domain height and the height profiles exhibited a higher corrugation after the antibody binding. Quantitative information were obtained by the analysis of the rms

surface roughness. In particular, the rms surface roughness of the membrane micro-domains, measured on 50x50 nm^2 square areas, increased from 0.25 ± 0.03 nm (mean ± SD; n = 11) to 0.34 ± 0.03 nm (mean ± SD; n = 11) after the antibody binding.

The experimental data pointing out the effect induced by the antibody specific binding suggest the presence of flotillin-1 in the membrane micro-domains. Moreover, the flotillin-1 recognition, a lipid raft-associated protein [20], and its high content in these membrane micro-domains strongly support the hypothesis that the areas visualized in the AFM images and protruding from the membrane patch surface could be identified as lipid rafts.

4. DISCUSSION AND CONCLUSIONS

Lipid rafts, small and highly dynamic micro-domains enriched in SM and CHOL located in the native biological membranes [1, 2], are suggested to play a significant role in many cellular processes such as membrane trafficking, signal transduction and regulation of membrane protein activity [1, 6, 7].

Many experimental tools have been used to identify lipid rafts and to clarify their physiological significance even if, till now, their existence is still a contentious topic. Along with specific antibodies for detecting raft proteins, bacterial toxins that target lipid components are often used as raft markers [27-29]. AFM has been shown to be a very useful technique to visualize and quantitatively characterize the topology of biological membranes also in physiological-like conditions [17-19]. In the present study we applied tapping mode AFM imaging to investigate lipid rafts of MDA-MB-231 human breast cancer cells. ~~using extraction with Triton X-100 followed by ultracentrifugation on sucrose gradient.~~ In tapping mode AFM the tip, mounted at the end of a cantilever vibrating at its resonant frequency, is placed near the sample and taps the surface only at the end of each oscillation cycle. The cantilever amplitude is held constant by altering the vertical position of the scanner. The topography image is then computed from the changes in scanner vertical position. Because the tip only makes intermittent contact with the sample, the lateral forces applied to the surface during the scanning are reduced and so tapping mode AFM is a very efficient imaging mode to study soft samples such as biological macromolecules and bio-membranes. Morpho-dimensional AFM analysis was also coupled with WB and HP-TLC assays to obtain a biochemical characterization of the structures visualized in AFM images. Membrane patches of MDA-MB-231 cell resistant to Triton X-100 extraction were purified by ultracentrifugation on a discontinuous sucrose gradient. All the 11 isolated fractions were analysed with respect to their flotillin-1 content by SDS-PAGE and WB assays. Fractions 5 and 6 showed the highest levels of flotillin-1, a lipid raft associated protein [20], as reported in Figure 1. Moreover, HP-TLC analysis

detected in the same purified fractions the highest content of CHOL and SM, lipids highly present in lipid rafts (see Figure 2). The biochemical data therefore confirm a larger presence of lipid rafts in the low-density fractions 5 and 6 corresponding to the 5% and 30% sucrose interface. In agreement with biochemical analyses, AFM imaging visualized large and planar membrane patches with lateral sizes of a few microns and an height of about 4-5 nm, as awaited for single lipid bilayers, only in the fractions with the richest content of flotillin-1, CHOL and SM (see Figure 3). Moreover, the number of the membrane patches decreases from fraction 5 to 7 as well as the flotillin-1, CHOL and SM content.

Classical preparation of lipid rafts uses 1% Triton X-100 to extract detergent resistant membranes which are then separated by ultracentrifugation on 5%-30% sucrose density gradient. Recently, different methods have been developed using a variety of other detergents or with detergent free techniques [30]. Some observations raised the hypothesis that treatment of cells with detergents may generate clusters of raft lipids and proteins that did not exist in the intact cells. Our data showed in fractions 5 and 6 the presence of membrane patches of 1-3 μm that may be formed through a mechanism of coalescence as a result of detergent treatment. Nevertheless recent data demonstrated that Triton X-100 does not induce domain formation or increase the fraction of the bilayer in the ordered state, although it does increase domain size by coalescing pre-existing domains [30]. Thus our observations are in agreement with this theory.

Interestingly high resolution AFM imaging of samples prepared from fraction 5 showed micro-domains protruding from the membrane patches by 1-2 nm and with lateral dimensions in the range of 100-500 nm in line with the range expected for lipid rafts [23, 24] as shown in Figures 4 and 5. In addition, while the surrounding membrane appears to be very smooth (rms surface roughness = 0.11 ± 0.01 nm; mean ± SD, n = 15), the micro-domain exhibits a surface corrugation (rms surface roughness = 0.26 ± 0.03 nm; mean ± SD, n = 18) with nanometer features on its surface which resemble proteins in both size and shape (see Figure 6).

The incubation of membrane patches with anti flotillin-1 antibody proved the protein nature of the structures visualized on the micro-domain surface as well as the presence of flotillin-1 among these proteins. In fact, as reported in Figure 7, just after 60 min of anti flotillin-1 antibody treatment the micro-domains changed their size and appearance showing an evident enlargement of the surface area. In particular the micro-domain surface area increased by about 20% while membrane patches showed an average increase of only about 8% (see Figure 8). ~~Besides,~~ The observed difference was statistically significant (t-Student's test: $P < 0.01$). Besides, membrane micro-domains exhibited a higher surface corrugation after the antibody binding and their rms surface roughness increased from 0.25 ± 0.03 nm (mean ± SD; n = 11) to 0.34 ± 0.03 nm (mean ± SD; n = 11).

On the contrary, control experiments carried out using anti clathrin hc, a non specific antibody raised against a non raft protein marker [25], showed an average increase of the surface area of about 8% for micro-domains as well as for membrane patches (see Figure 8). The increase of the membrane patch surface area, of the same order both in the anti flotillin-1 treated and control experiments, could be caused by re-aggregation processes of lipid aggregates not well adhered to the mica support.

Interestingly, the increase of the surface area of the membrane micro-domains induced by the anti flotillin-1 treatment showed values distributed in two different ranges, 8-10% and 24-27%. These differences can be justified taken in account that the sample preparation protocol for AFM imaging does not allow to select the orientation of the membrane patches on the mica support. Since anti flotillin-1 binds to the cytoplasmic side of the plasma membrane, the 8-10% surface area increase could be induced by non specific physisorption phenomena on micro-domains exposing the external face of the membrane. As a result the increase of the micro-domain surface area of about 20% induced by the anti flotillin-1 antibody binding could be an underestimation of the real value.

~~On the contrary, control experiments carried out imaging membrane patches in recording buffer, after 60 min showed an average increase of the surface area of about 8% for micro-domains as well as for membrane patches (see Figure 8). The increase of the membrane patch surface area, of the same order both in the antibody treated and control experiments, could be caused by re-aggregation processes of lipid aggregates not well adhered to the mica support.~~

4.1 Concluding remarks

Taken together the biochemical data as well as the flotillin-1 recognition and its high content in the membrane micro-domains, strongly indicate that the nanometer areas protruding from the membrane patch surface and visualized in AFM images are lipid rafts. Moreover, our results are in favourable agreement with data reported in literature and obtained using different experimental approaches [2, ~~10~~]. We believe that further applications of AFM imaging to lipid raft topic in both healthy and pathological native biological membranes coupled with a detailed biochemical investigation could contribute to better understanding some basic properties and molecular mechanisms of this important biological phenomenon.

ACKNOWLEDGEMENTS

The authors thank the Banca del Monte di Lombardia Foundation for its support for AFM instrumentation purchasing. This work was supported by ASI (MoMa) grant to A.M.R.

REFERENCES

[1] K. Simons and E. Ikonen, Functional rafts in cell membranes, Nature 387 (1997) 569–572.

[2] K. Simons and W.L. Vaz, Model systems, lipid rafts, and cell membranes, Annu. Rev. Biophys. Biomol. Struct. 33 (2004) 269–295.

[3] D.A. Brown, E. London, Functions of lipid rafts in biological membranes, Annu Rev Cell Dev Biol. 14 (1998) 111–36.

[4] A.S. Shaw, Lipid rafts: now you see them, now you don't, Nat. Immunol. 7 (2006) 1139–42.

[5] L.J. Foster, C.L. De Hoog, M. Mann, Unbiased quantitative proteomics of lipid rafts reveals high specificity for signaling factors, Proc. Natl. Acad. Sci. USA 100 (2003) 5813–8.

[6] S. Mayor and M. Rao, Rafts: scale-dependent, active lipid organization at the cell surface, Traffic 5 (2004) 231–240.

[7] M. Edidin, The state of lipid rafts: From model membranes to cells, Annu Rev Biophys Biomol Struct 32 (2003) 257–283.

[8] E. London, How principles of domain formation in model membranes may explain ambiguities concerning lipid raft formation in cells, Biochim. Biophys. Acta 1746 (2005) 203–220.

[9] P.F.F. Almeida, A. Pokorny, A. Hinderliter, Thermodynamics of membrane domains, Biochim. Biophys. Acta 1720 (2005) 1–13.

~~[10] K. Gaus, E. Gratton, E.P.W. Kable, A.S. Jones, I. Gelissen, L. Kritharides and W. Jessup, Visualizing lipid structure and raft domains in living cells with two-photon microscopy, Proc. Natl. Acad. Sci. USA 100 (2003) 15554–15559.~~

[10] S.W. Hell, J. Wichmann, Breaking the diffraction resolution limit by stimulated emission: Stimulated emission depletion microscopy, Opt. Lett. 19 (1994) 780–782.

[11] C. Eggeling, C. Ringemann, R. Medda, G. Schwarzmann, K. Sandhoff, S. Polyakova, V.N. Belov, B. Hein, C. von Middendorff, A. Schonle and S.W. Hell, Direct observation of the nanoscale dynamics of membrane lipids in a living cell, Nature 457 (2009) 1159–1163.

[12] C. Ringemann, B. Harke, C. von Middendorff, R. Medda, A. Honigmann, R. Wagner, M. Leutenegger, A. Schonle, S.W. Hell and C. Eggeling, Exploring single-molecule dynamics with fluorescence nanoscopy, New J. Phys. 11 (2009) 103054.

[13] S.J. Sahl, M. Leutenegger, M. Hilbert, S.W. Hell and C. Eggeling, Fast molecular tracking maps nanoscale dynamics of plasma membrane lipids, Proc. Natl. Acad. Sci. USA 107 (2010) 6829-6834.

[14] P. Sengupta, T. Jovanovic-Talisman, D. Skoko, M. Renz, S.L Veatch, J. Lippincott-Schwartz, Probing protein heterogeneity in the plasma membrane using PALM and pair correlation analysis, Nature Methods 8 (2011) 969-975.

[15] H. Mizuno, M. Abe, P. Dedecker, A. Makino, S. Rocha, Y. Ohno-Iwashita, J. Hofkens, T. Kobayashi, A. Miyawaki, Fluorescent probes for superresolution imaging of lipid domains on the plasma membrane, Chemical Science 2 (2011) 1548-1553.

[16] C.R. Anderton, K. Lou, P.K. Weber, I.D. Hutcheon, M.L. Kraft, Correlated AFM and NanoSIMS imaging to probe cholesterol-induced changes in phase behaviour and non-ideal mixing in ternary lipid membranes, Biochim. Biophys. Acta 1808 (2011) 307-315.

[17] B.W. Hoogenboom, K. Suda, A. Engel, D. Fotiadis, Supramolecular assemblies of the voltage-dependent anion channel in the native membrane, J. Mol. Biol. 370 (2007) 246–255.

[18] D.J. Muller, A. Engel, Conformational changes, flexibilities and intramolecular forces observed on individual proteins using AFM, RIKEN Rev. 36 (2001) 29–31.

[19] S. Scheuring, AFM studies of the supramolecular assembly of bacterial photosynthetic core-complexes, Curr. Opin. Chem. Biol. 10 (2006) 387–393.

[20] L.J. Pike, Lipid rafts: bringing order to chaos, J. Lipid Research 44 (2003) 655-667.

[21] P.K. Hansma, J.P. Cleveland, M. Radmacher, D.A. Walters, P.E. Hillner, M. Bezanilla, M. Fritz, D. Vie, H.G. Hansma, C.B. Prater, Tapping mode atomic-force microscopy in liquids, Appl. Phys. Lett. 64 (1994) 1738–1740.

[22] N. Buzhynskyy, C. Salesse and S. Scheuring, Rhodopsin is spatially heterogeneously distributed in rod outer segment disk membranes. J. Mol. Recognit, 24 (2011) 483–489.

[23] G.J. Schütz, G. Kada, V.Ph. Pastushenko and H. Schindler, Properties of lipid microdomains in a muscle cell membrane visualized by single molecule microscopy, The EMBO J. 19 (2000) 892-901.

[24] D. Lingwood and K. Simons, Lipid Rafts as a Membrane-Organizing Principle, Science 327 (2010) 46-50.

[25] N. Fabelo, V. Martin, G. Santpere, R. Marin, L. Torrent and M. Diaz, Severe alterations in lipid composition of frontal cortex lipid rafts from Parkinson's disease and incidental Parkinson's disease, Molecular Medicine 17 (2011) 1107–1118.

[26] D.J. Muller, C.A. Schoenenberger, G. Buldt and A. Engel, Immuno-Atomic Force Microscopy of Purple Membrane, Biophysical J. 70 (1996) 1796-1802.

[27] R.G. Parton, Ultrastructural localization of gangliosides; GM1 is concentrated in caveolae, J. Histochem. Cytochem. 42 (1994) 155–166.

[28] M. Fivaz, L. Abrami, F.G. van der Goot, Landing on lipid rafts, Trends Cell Biol. 9 (1999) 212–213.

[29] A. Yamaji, Y. Sekizawa, K. Emoto, H. Sakuraba, K. Inoue, H. Kobayashi, M. Umeda, Lysenin, a novel sphingomyelin-specific binding protein, J. Biol. Chem. 273 (1998) 5300–5306.

[30] P. Pathak, E. London, Measurement of lipid nanodomain (raft) formation and size in sphingomyelin/POPC/cholesterol vesicles shows TX-100 and transmembrane helices increase domain size by coalescing preexisting nanodomains but do not induce domain formation, Biophysical J. 101 (2011) 2417-2425.

FIGURE CAPTIONS

Figure 1.

Distribution of flotillin-1 in Triton X-100 isolated MDA-MB-231 human breast cancer cell membranes. Triton X-100 lysates of cell cultures were purified and fractionated by sucrose gradient ultracentrifugation. Equal volumes of each fraction were analysed by Western Blotting with antibodies to flotillin-1 protein. Fractions 5 and 6 have the highest flotillin-1 content.

Figure 2.

*Distribution of CHOL (**a**) and SM (**b**) content in Triton X-100 isolated MDA-MB-231 human breast cancer cell membranes. Triton X-100 lysates of cell cultures were purified and fractionated by sucrose gradient ultracentrifugation. Equal volumes of each fraction were analysed by HP-TLC. Fractions 5 and 6 have the highest content of CHOL and SM.*

Figure 3.

AFM topography images of some isolated fractions. Purified membranes were diluted 1:30 in distilled water and 50 μl of the suspension placed on a mica support. AFM images were collected in liquid buffer in tapping mode. Different situations were visualized: membrane patches with lateral sizes of a few microns and height of 4 nm (fractions from 5 to 7), small membrane fragments (fractions from 1 to 4, 8 and 9) and an homogeneous distribution of membrane fragments on the whole support (fractions 10 and 11). For all the images: scan area = 10x10 μm^2; z range (from darkest to lightest) = 20 nm; scale bar = 1 μm.

Figure 4.

AFM topography image of a membrane sample prepared from fraction 5 collected in liquid buffer in tapping mode. Different regions are visualized: the mica support (1), a membrane patch (2), two micro-domains protruding from the membrane surface (3) and higher aggregates (white areas).
Scan area = 1.5x1.5 μm^2; z range (from darkest to lightest) = 15 nm.

Figure 5.

*(**left**) AFM topography image of a membrane sample prepared from fraction 5 and collected in liquid buffer in tapping mode. The image shows a membrane patch 4 nm thick (green arrows) with two micro-domains and some protein aggregates (brighter areas). (**right**) Height profile corresponding to the black line drawn in AFM image. The micro-domain protrudes by 2 nm from the membrane surface (red arrows). Scan area = 1.6x1.6 μm^2; z range (from darkest to lightest) = 20 nm.*

Figure 6.

*(**left**) High resolution AFM topography image of a membrane sample prepared from fraction 5 and collected in liquid buffer in tapping mode. The image shows a micro-domain (1) which protrudes by about 1 nm from the surface (2) of the membrane patch (red arrows). The micro-domain has a surface roughness while the surrounding membrane is very smooth. (**right**) Height profile corresponding to the black line drawn in AFM image. Nanometer features are visible on the micro-domain surface comparable for dimensions with proteins. Scan area = 200x200 nm^2; z range (from darkest to lightest) = 2 nm.*

Figure 7.

*AFM topography images of membrane samples prepared from fraction 5 and collected in liquid buffer in tapping mode. Untreated membrane patches (**a**) were incubated with anti flotillin-1 antibody (1:4 in adsorption buffer) for different times (0, 30, 60 min). Just after 60 min of treatment (**b**) the surface area of micro-domains protruding from the membrane patches clearly increases (see circled areas) thus suggesting the presence of flotillin-1 proteins. Scan area = 5x5 μm^2; z range (from darkest to lightest) = 25 nm.*

Figure 8.

Histogram of the surface area increase for membrane patches, ~~7.9 ± 1.5% (mean ± SD; n = 10)~~ 8.3 ± 2.4% (mean ± SD; n = 10), and micro-domains, ~~17.8 ± 6.1% (mean ± SD; n = 12)~~ 20.7 ± 5.6% (mean ± SD; n = 11), after 60 min anti flotillin-1 antibody incubation (gray bars) and of the surface area increase for membrane patches~~, 8.8 ± 1.9% (mean ± SD; n = 10)~~ 9.4 ± 2.5% (mean ± SD; n = 10), and micro-domains, ~~6.7 ± 1.7% (mean ± SD; n = 10)~~ 8.1 ± 1.6% (mean ± SD; n = 10), in the control experiment after 60 min anti clathrin hc antibody incubation (white bars). The observed difference among the surface area increase of the micro-domains, induced by the anti flotillin-1 ~~antibody~~ treatment, and of membrane patches both in the anti flotillin-1 ~~antibody~~ treated and control experiment as well as of the micro-domains in the control experiment is statistically significant (t-Student's test: P < 0.01).

Figure1

Click here to download high resolution image

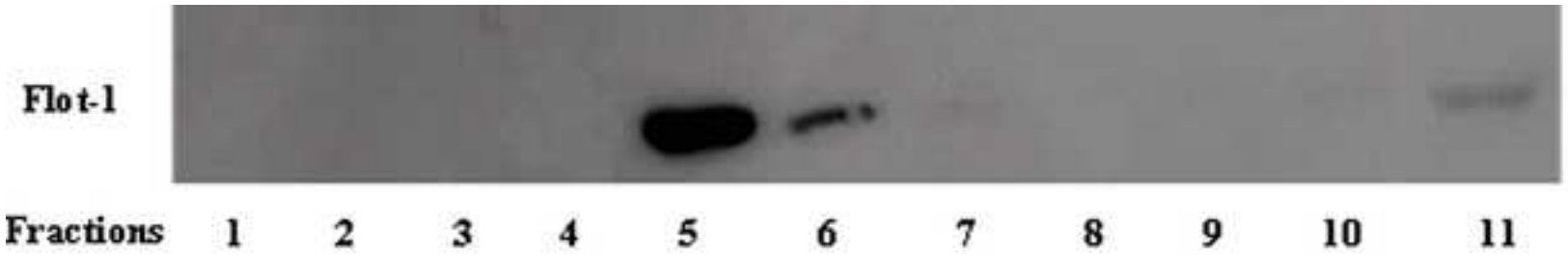

Figure2

Click here to download high resolution image

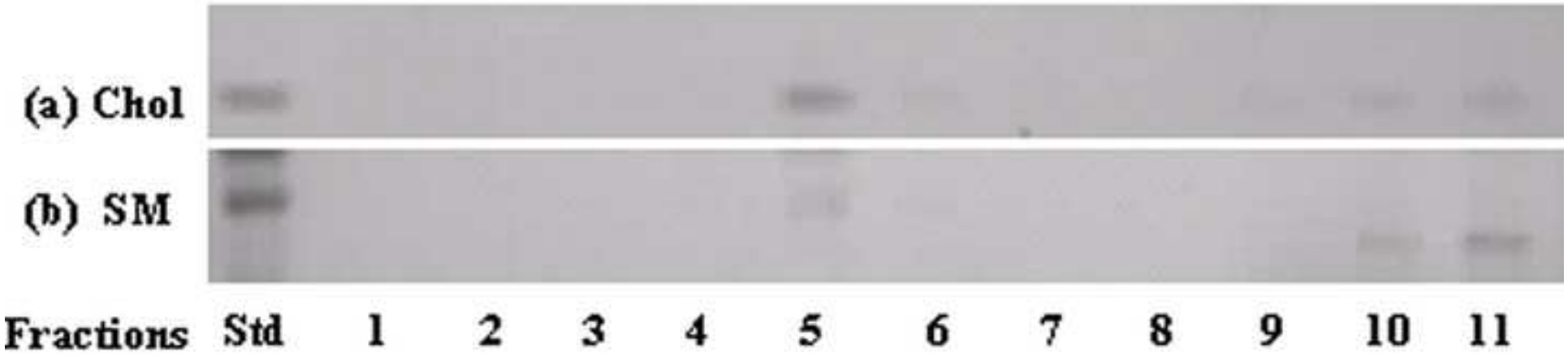

Figure3

Click here to download high resolution image

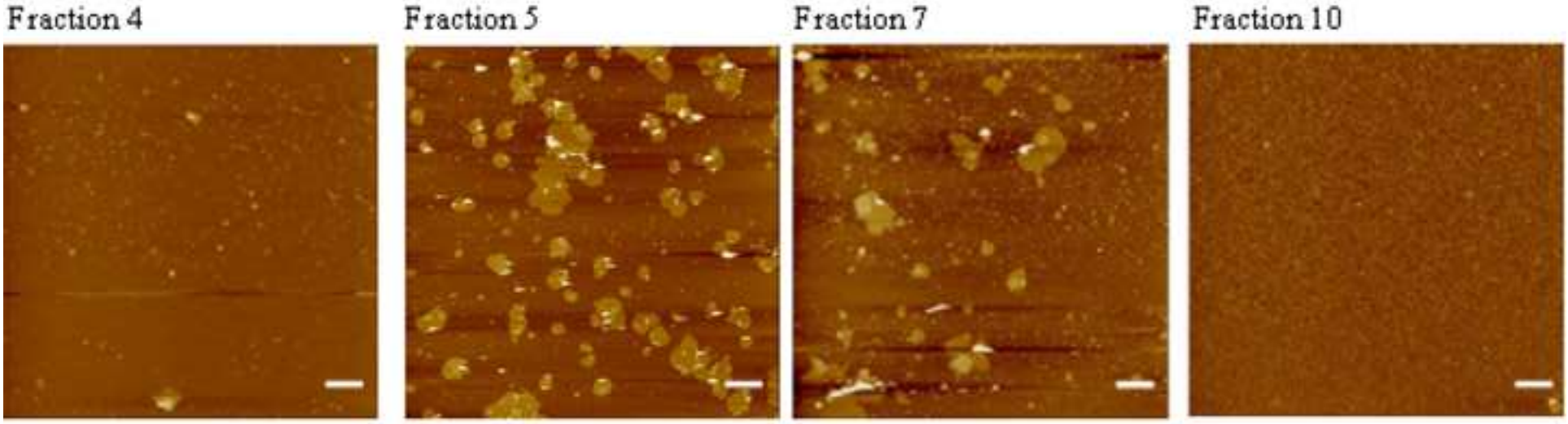

Figure4

Click here to download high resolution image

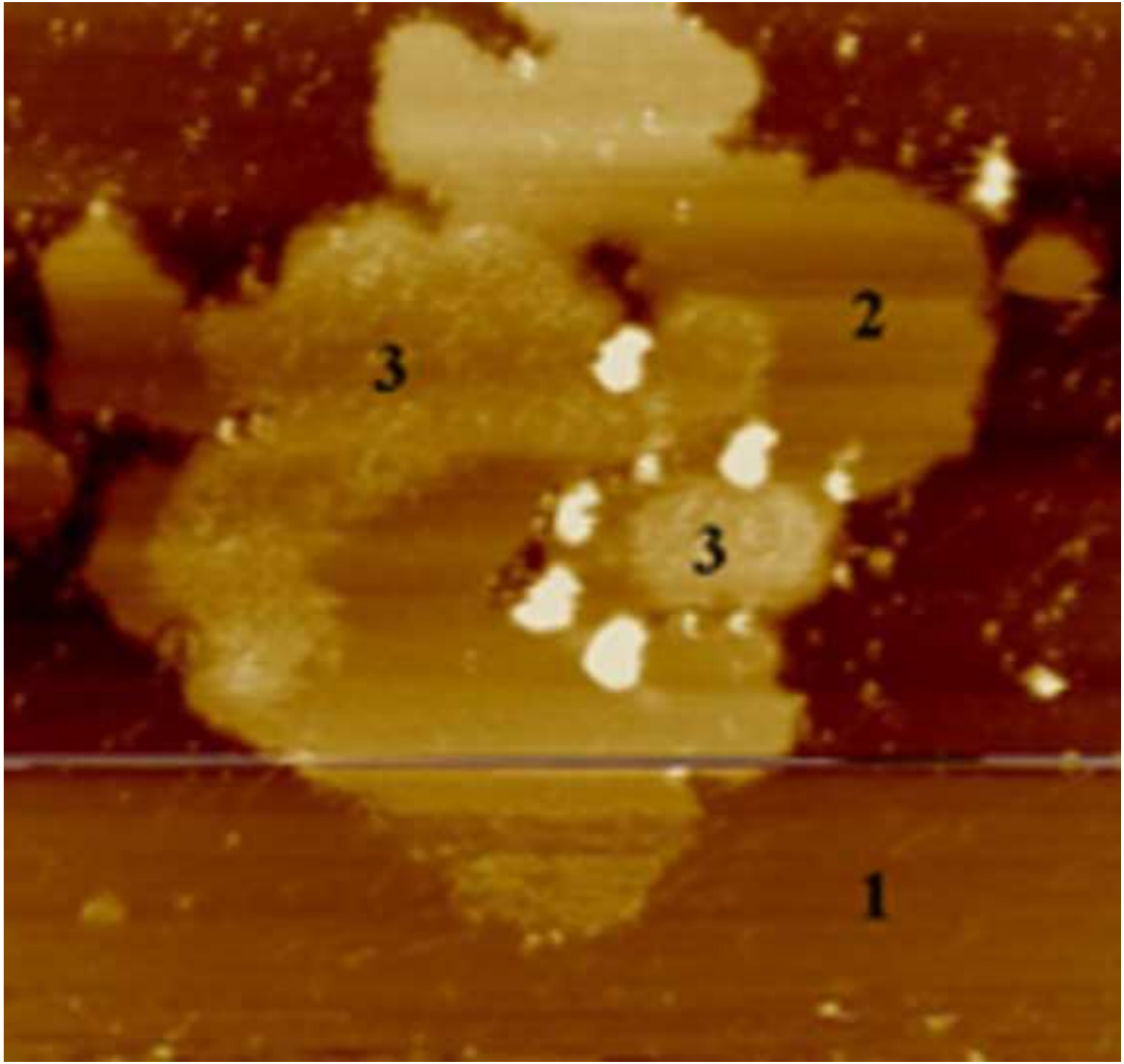

Figure5

Click here to download high resolution image

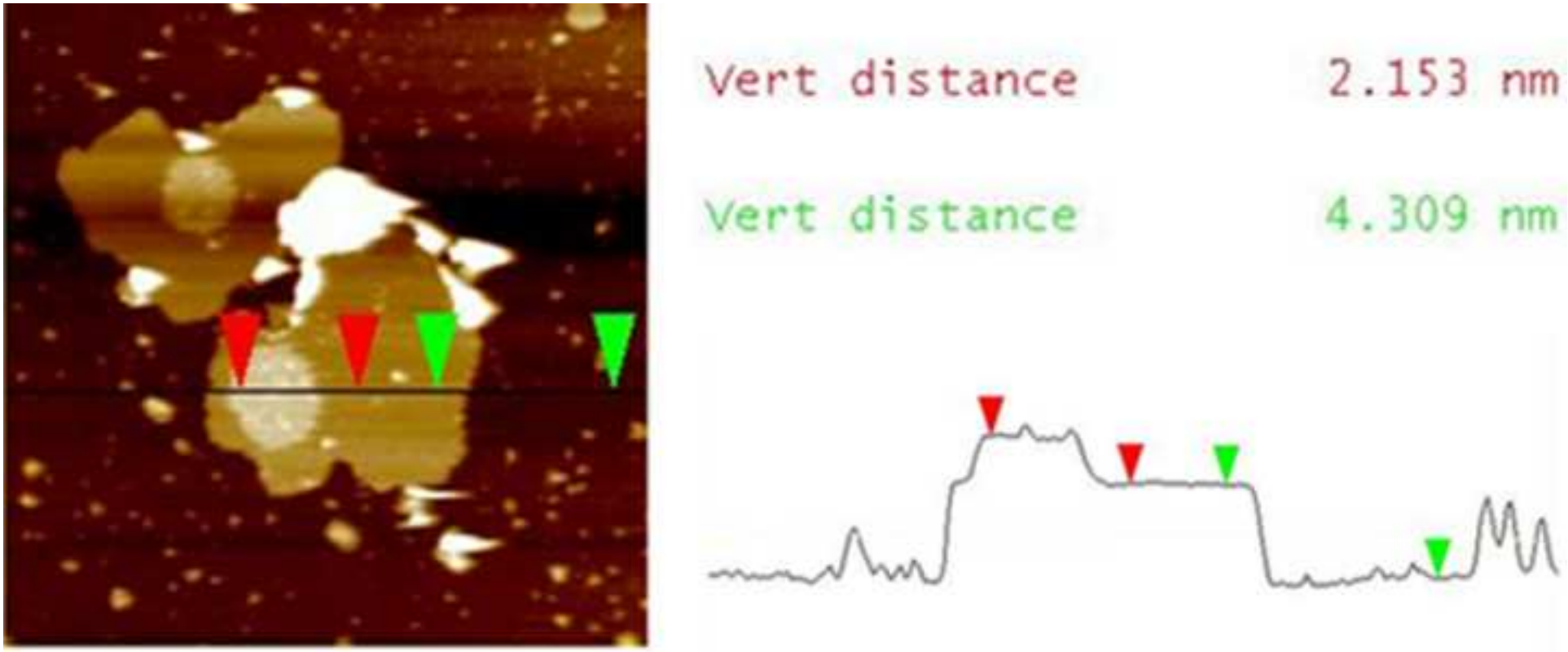

Figure6

Click here to download high resolution image

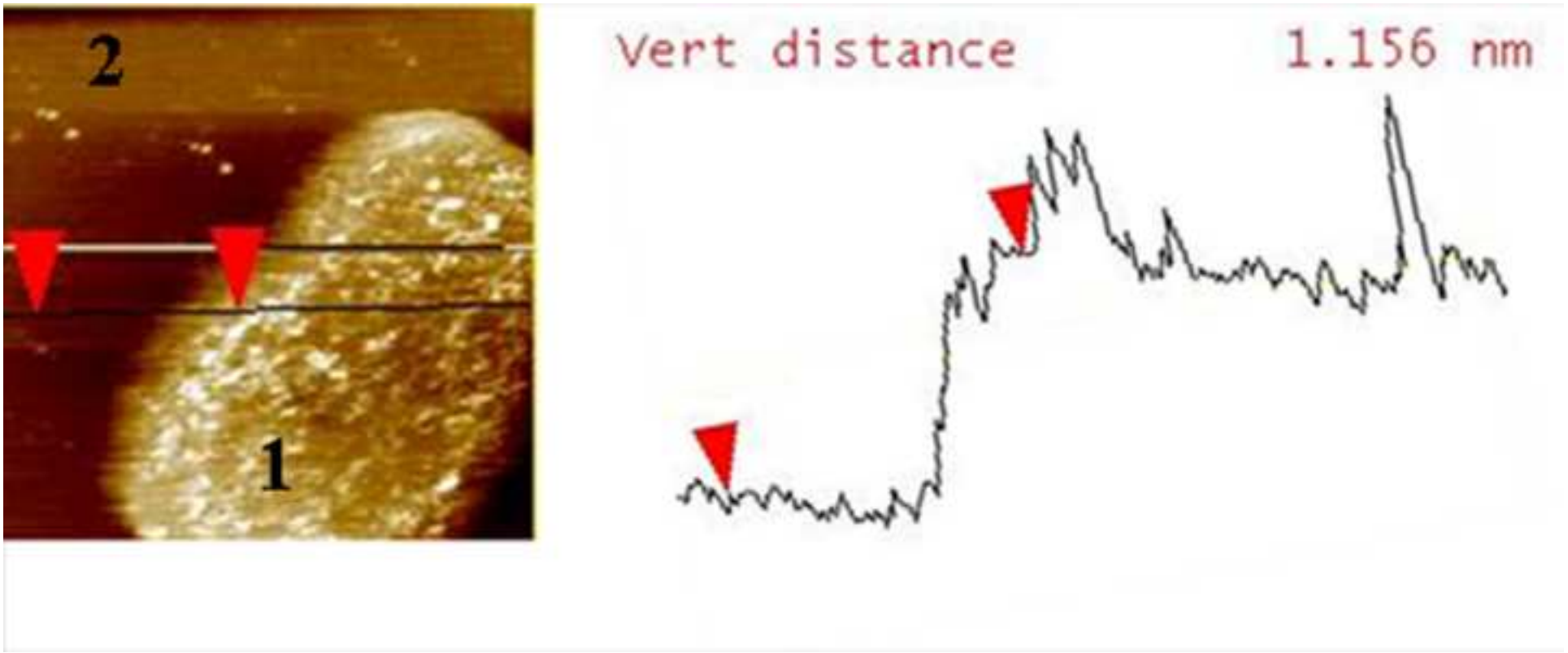

Figure7

Click here to download high resolution image

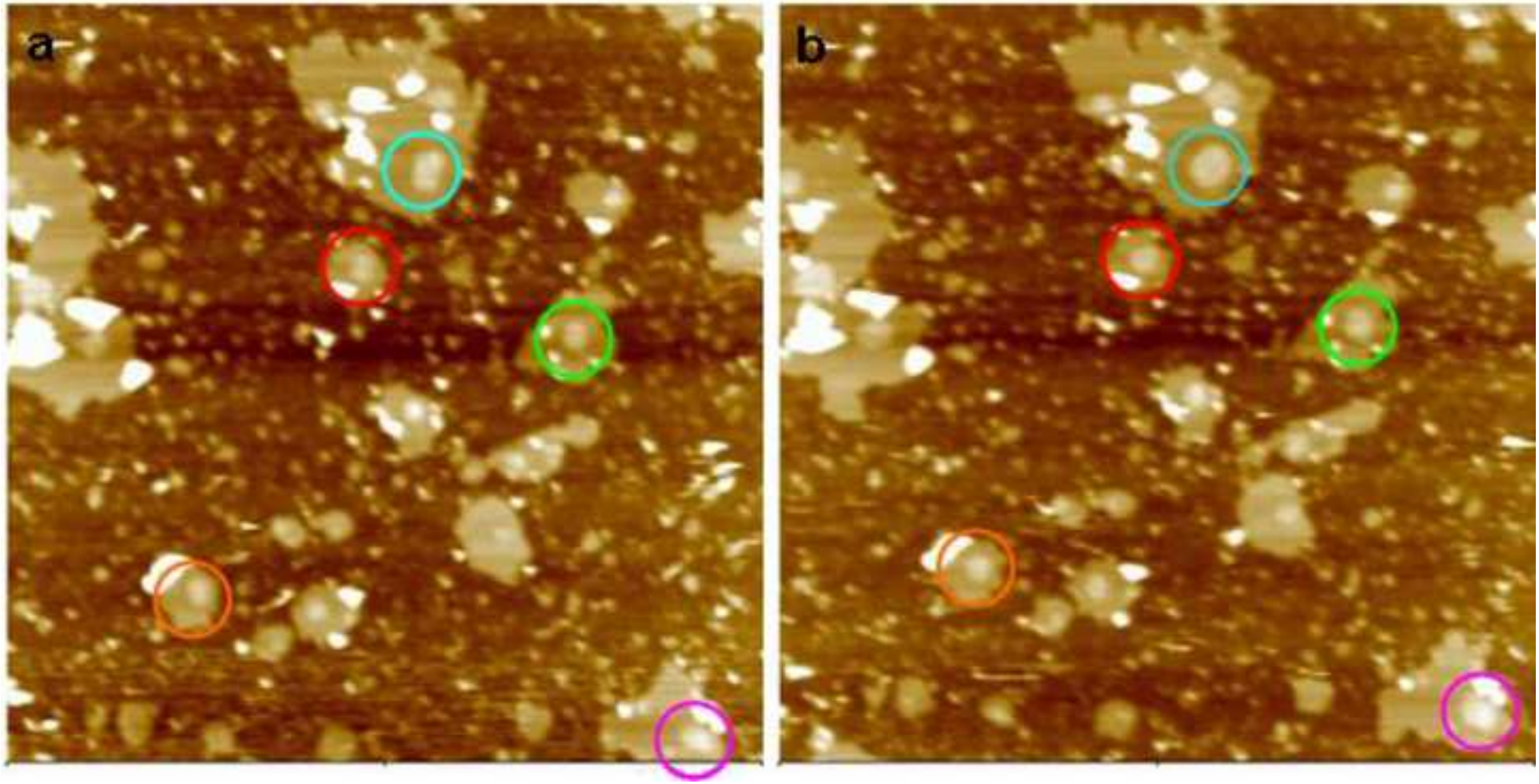

Figure8

Click here to download high resolution image